INVESTIGATION OF NITROUS OXIDE BIOSYNTHESIS BY A BACTERIAL NITRIC OXIDE REDUCTASE (NOR) AND AN ENGINEERED NOR MIMIC USING STABLE ISOTOPE RATIO MASS SPECTROMETRY

By

Clarisse Marie Finders

A THESIS

Submitted to
Michigan State University
in partial fulfillment of the requirements
for the degree of

Biochemistry and Molecular Biology—Master of Science

2018

ABSTRACT

INVESTIGATION OF NITROUS OXIDE BIOSYNTHESIS BY A BACTERIAL NITRIC OXIDE REDUCTASE (NOR) AND AN ENGINEERED NOR MIMIC USING STABLE ISOTOPE RATIO MASS SPECTROMETRY

By

Clarisse Marie Finders

While carbon dioxide (CO_2) is the most prevalent greenhouse gas, nitrous oxide (N_2O) is far more potent, with a global warming potential ~265 times greater than that of carbon dioxide over a 100-year period.[1] Additionally, N_2O is capable of destroying ozone, making it doubly concerning as a greenhouse gas. Approximately half of the N_2O produced yearly is from anthropogenic sources. The largest contributor to anthropogenic N_2O is the over-fertilization of agricultural soils, which fuels a host of microbial nitrogen cycling processes that produce N_2O. One of these processes is denitrification, and N_2O is known to be an obligate intermediate in this process. In denitrification, N_2O is synthesized by an enzyme known as nitric oxide reductase (NOR). A thorough understanding of the enzymatic mechanisms by which N_2O is produced is essential to mitigating anthropogenic N_2O emissions. To this end, this thesis contains the examination of N_2O produced by a bacterial cytochrome *c* NOR (cNOR) from *Paracoccus dentrificans* and a cNOR mimic, I107EFe_BMb, using stable isotope ratio mass spectrometry (IRMS). The first chapter provides the reader with an introduction to the nitrogen cycle, the known NORs, and the basics of isotope theory. The studies on the native cNOR and I107EFe_BMb are contained in the second and third chapters, respectively. Conclusions and future directions are presented in the final chapter.

This thesis is dedicated to Eric Hegg, who saw my potential as a scientist, welcomed me into his lab, and gave me guidance along the way; to Joshua Haslun, who challenged me to become what Eric could see; to Aaron Mebane, Kathleen Thompson, Stephen, Mary, John, Victoria, and James Finders, who encouraged me and listened to me; and finally to Elise Rivett, who put up with me asking “What color does this look like to you?” for three years and shared the laughter and trials of daily life lab with me.

ACKNOWLEDGEMENTS

I would like to acknowledge Hasand Ghandi for his assistance with samples and insight into experiments and isotopic data, and Peggy and Nathaniel Ostrom for their insights and allowing me to use their instruments and Nathaniel Ostrom and Bob Hausinger for agreeing to be my committee members. I would also like to acknowledge Yi Lu, Julian Reed, and Pia Ädelroth for generously providing purified enzyme, as well as Nicolai Lehnert, Jennifer Dubois, and Judith Klinman for their helpful discussions and insights.

TABLE OF CONTENTS

LIST OF TABLES

LIST OF FIGURES

KEY TO SYMBOLS AND ABBREVIATIONS

α Fractionation factor

δ delta

ε Isotopic enrichment factor

η Net isotope effect

ν Frequency

Anammox Anaerobic ammonia oxidation

AOA/B Ammonia Oxidizing Archaea/Bacteria

BNC Binuclear center

BNF Biological Nitrogen Fixation

CO_2 Carbon dioxide

Comammox Complete ammonia oxidation

DFT Density Functional Theory

DNRA Dissimilatory Nitrate Reduction to Ammonia

ECD Electron Capture Detector

EPR Electron Paramagnetic Resonance

EXC Excited states

FeMo-co Iron-molybdenum cofactor

FMN Flavin mononucleotide

FNOR/FIRd Flavorubredoxin

HAO Hydroxylamine oxidoreductase

HCO Heme Copper Oxidases

Hcp Hybrid cluster protein

HNO_3 Nitric acid

KIE Kinetic Isotope Effect

KIE_{int} intrinsic KIE

KIE_{obs} observed KIE

LSR Least Squares Regression

Mb myoglobin

MMI Mass Moment of Inertia

N_2 Dinitrogen

N_2O Nitrous oxide

Nar Nitrate reductase

NH_3 Ammonia

NH_2OH Hydroxylamine

Nir Nitrite reductase

NO_2^- Nitrate

NO_3^- Nitrate

NO_x Nitric oxides

NOB Nitrate Oxidizing Bacteria

NOR Nitrous Oxide Reductase

Nos Nitrous oxide reductase

N_r Reactive Nitrogen Species

NXR Nitrate Oxidoreductase

qNOR quinol Nitric Oxide Reductase

RLM Robust Linear Modeling

S_P Site Preference

TG-IRMS Trace Gas Isotope Ratio Mass Spectrometry

TS Transition State

TSDF Transition State Decomposition Frequency

UV-Vis Ultra violet-visible

ZnPP Zinc protoporphyrin IX

ZPE Zero Point Energy

CHAPTER 1: Nitrogen, NORs, and Navigating Stable Isotopes

Introduction to the nitrogen cycle

Nitrogen is an essential element to life due to its presence in amino acids and nucleic acids. The nitrogen cycle, as the name implies, is the circulation of nitrogen species in the atmosphere, landmasses, and bodies of water. All nitrogen species fall into one of two categories: largely inert dinitrogen (N_2) or reactive nitrogen species (N_r). N_2 and N_r are linked together in a triangle with the three vertices as N_2, nitrate (NO_3^-) as the most oxidized N_r, and ammonia (NH_3) as the most reduced N_r. These three nitrogen species are interconverted through a host of biochemical processes that produce other N_r intermediates including hydroxylamine (NH_2OH), nitric acid (HNO_3), nitrite (NO_2^-), nitrogen oxides (NO_x), and nitrous oxide (N_2O) (Figure 1).[2] One technique that has proven to be highly useful in elucidating transformations within the nitrogen cycle is stable isotope tracing.[3] Stable isotopes are atoms of the same element that differ in mass only and are not radioactive. By examining the rate of the reaction for either ^{14}N (more common isotope) or ^{15}N (less common isotope), it is possible to assign isotopic identifiers (called isotopic enrichment factors, discussed later) to a process. This is particularly helpful in field studies where multiple nitrogen cycling processes occur simultaneously.

As the marine and atmospheric nitrogen cycles are reviewed elsewhere,[2,4] the scope of this chapter is limited to the terrestrial nitrogen cycle. Basic information needed to understand isotopic measurements is presented first. The known processes in the terrestrial nitrogen cycle

are discussed, as well as a brief mention of any relevant stable isotope studies. Particular attention is given to N_2O as a greenhouse gas and the current state of knowledge of the enzymes that produce it. Finally, the theory of using stable isotopes to gain enzymatic mechanistic insights is also presented.

Isotope notation

Isotopes are traditionally measured as ratios with the isotopic ratio R defined as the abundance of the heavy isotope over the abundance of the light isotope:

$$R = \frac{\text{Heavy Isotope}}{\text{Light Isotope}} = \frac{^{15}N}{^{14}N} \quad (1)$$

To enable standardization and comparison of isotopic measurements, R is converted to the delta (δ) notation:

$$\delta = \left(\left(\frac{R_{sample}}{R_{standard}}\right) - 1\right) * 1000 \quad (2)$$

where R_{sample} is the isotope ratio of the sample and $R_{standard}$ is the isotope ratio of the international standard. The international standards for $\delta^{15}N$ is atmospheric N_2.[5]

Many reactions in the nitrogen cycle react with the two N isotopes at different rates.[3] The ratio of these rates is known as the fractionation factor, symbolized by α:

$$\alpha = \frac{k_2}{k_1} \quad (3)$$

where k_2 is the reaction rate for the heavy isotope and k_1 is the reaction rate for the light isotope. While α can be measured directly, it can also be derived from the isotopic enrichment factor, ε.[6]

$$\varepsilon = (\alpha - 1) * 1000 \quad (4)$$

The term ε can be obtained in several ways, one of which is Mariotti's approximation of the Rayleigh equation:[7]

$$\delta_{\text{product}} = \delta_{\text{sample}} - \varepsilon_{\frac{\text{Product}}{\text{Substrate}}}\left(\frac{f*\ln f}{1-f}\right) \quad (5)$$

where *f* is the fraction of the substrate remaining in the reaction. Eqn. 5 is most accurate for a unidirectional single step reaction in a closed system. This encompasses some enzymatic assays, but not experiments that measure an entire process involving multiple reactions, such as pure culture studies or field sampling. For these studies, η, which is a net isotope effect, is given. A net isotope effect is the isotope effect of a multistep process that contains observable intermediates. For example, a net isotope effect would be observed for a monoculture study on nitrification as NH_3 is oxidized to NO_3^- with NH_2OH as an intermediate. In this manuscript, a negative ε or η indicates a preference for the light isotope in the product while a positive ε or η indicates preferential incorporation of the heavy isotope.

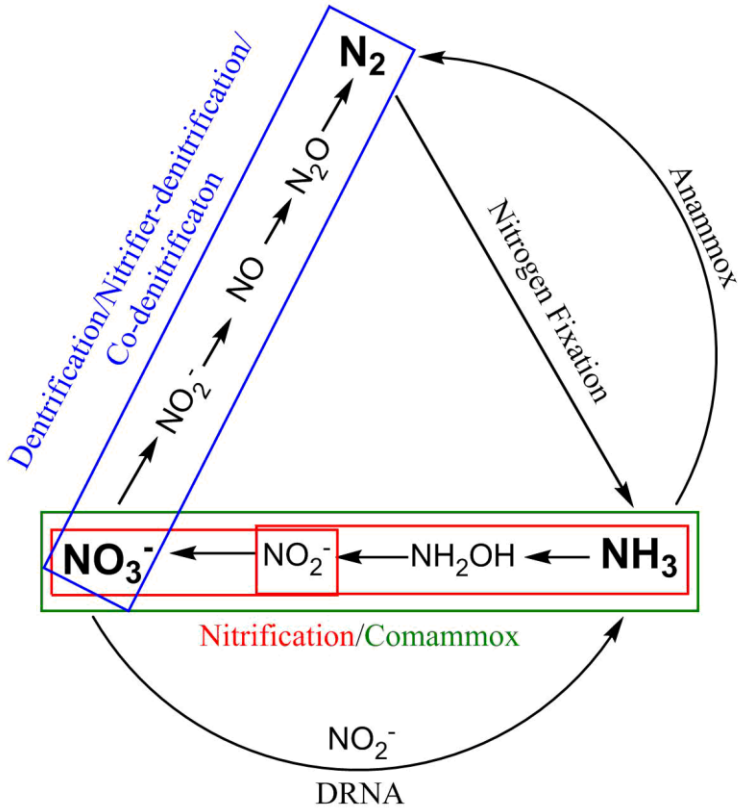

Figure 1. Diagram of the nitrogen cycle. Nitrogen fixation occurs when N_2 is turned into NH_3. Anammox is the simultaneous oxidation of ammonia and reduction of nitrite to produce N_2 and water. Nitrification (red boxes) occurs in two stages: ammonia oxidizing archaea/bacteria (AOA/B) transform NH_3 to NH_2OH to NO to NO_2^-, and nitrite oxidizing bacteria (NOB) catalyze the formation NO_3^- from NO_2^-. Comammox (green box) is the same process as nitrification but performed entirely in one organism. Dissimilatory nitrate reduction to ammonia (DNRA) is the reverse process of nitrification and comammox. The three denitrification processes (blue box) enable conversion of oxidized N_r to N_2. Denitrification is the reduction of NO_3^- to N_2 via NO_2^-, NO, and N_2O. Nitrifier-denitrification is the same process, but performed by nitrifying bacteria and fungi. Co-denitrification is the utilization of co-substrates during denitrification, using an oxidized N_r (NO or N_2O) and a reduced N_r to form N_2O or N_2.

From N_2 to NH_3: Nitrogen fixation

The largest bioavailable nitrogen reservoir is the atmosphere, the vast majority of which is N_2. As N_r are continually being depleted through assimilation, sequestration, and conversion back to N_2, nitrogen fixation must be carried out constantly to sustain life.[8] Reduction of N_2 to N_r is difficult, requiring catalysis either by a specialized enzyme known as nitrogenase or industrially

by the Haber-Bosch process.[4] Biological nitrogen fixation (BNF) is performed by select microbes that synthesize the enzyme nitrogenase. Thus far, three different types of nitrogenases have been discovered, and are named for the metal found in the active site. These are molybdenum nitrogenase, vanadium nitrogenase, and iron nitrogenase.[9] As molybdenum nitrogenase is the most common nitrogenase, it is the only one discussed here. The molybdenum nitrogenase complex is a dimer of trimers, with one half of the enzyme containing an Fe protein that forms a dimer with an MoFe protein that contains an α and β subunit. Three distinct metal clusters are found in nitrogenase: the F cluster in the Fe protein, which is a [4Fe-4S] cluster, the P cluster in the β MoFe subunit ([8Fe-7S cluster]) and the iron-molybdenum cofactor (FeMo-co) in the α MoFe subunit, which serves as the catalytic site. The FeMo-co is an [Mo-7Fe-9S-C-homocitrate] cluster. This takes the form of two [4Fe-4S] clusters bound together in which the sulfur connecting the two clusters is replaced by a carbon atom and a terminal iron is replaced with Mo. Three sulfurs bridge the two clusters and the homocitrate coordinates the Mo.[8,10]

Stoichiometrically, nitrogenase catalyzes the reaction:

$$N_2 + 8\ e^- + 16\ ATP + 8\ H^+ \rightarrow 2\ NH_3 + H_2 + 16\ ADP + 16\ P_i$$

As evidenced by the large number of ATPs used, nitrogen fixation is a highly energy intensive process for the cell.[8]

Anthropogenic nitrogen fixation is also energetically expensive, with more than 1% of the energy produced in the world used for the Haber-Bosch process.[11] Developed between 1909 and 1913, the Haber-Bosch process converts N_2 and H_2 to NH_3 through the use of a catalyst, high heat, and pressure. While the conversion of N_2 and H_2 to NH_3 is an exothermic reaction, the natural rate at which this reduction occurs is not practical economically. Heat can be applied to

increase the rate of the reaction; because heat drives the equilibrium away from ammonia production, however, pressure is also needed to take advantage of Le Chatelier's principle and obtain the desired product. The Haber-Bosch process accounts for approximately two thirds of all terrestrial nitrogen fixation while BNF accounts for the remaining third.[4] There have been some stable isotope studies performed on BNF.[12,13] Zhang *et al.* used mutant strains that could express only one nitrogenase and observed that there was a slight discrimination against the heavier isotope (-6 to -7‰)[14] Taking all of the available data together indicates a slight discrimination against the heavy isotope (Average $\eta = -2.34 \pm 2.02$‰).[3]

NH_3 to NO_3^-/N_2: Nitrification, Comammox, and Anammox

Once N_2 is fixed as NH_3, another set of nitrogen transformations can begin, finishing with either NO_3^- or N_2 as the final product. These processes are known as nitrification, complete ammonia oxidation (comammox), and anaerobic ammonia oxidation (anammox).

Nitrification is the oxidation of ammonia or ammonium to nitrite or nitrate under aerobic conditions, and both chemotrophic nitrification and heterotrophic nitrification have been discovered.[15] Nitrification can be carried out by two different sets of microbes, ammonia oxidizing archaea/bacteria (AOA/B) and nitrate oxidizing bacteria (NOB).[16] The reactions in the pathway are shown below:[17,18]

$$NH_3 + O_2 + 2\ e^- + 2\ H^+ \rightarrow NH_2OH + H_2O$$

$$NH_2OH + H_2O \rightarrow NO + 3\ e^- + 3\ H^+ + H_2O$$

$$NO + 2\ OH^- \rightarrow NO_2^- + e^-$$

$$NO_2^- + H_2O \rightarrow NO_3^- + 3\ e^- + 2\ H^+$$

AOA/B catalyze the first set of reactions while NOB carry out the last step of converting nitrite to nitrate. The first reaction is catalyzed by an enzyme known as ammonia monooxygenase (AMO) while the conversion of NH_2OH to NO is performed by hydroxylamine oxidoreductase (HAO). Until recently it was thought that HAO oxidized hydroxylamine directly to nitrate. Caranto *et al.* definitively demonstrated that under both aerobic and anaerobic conditions, HAO produces NO as its final product rather than NO_2^-.[17] Other side products that can be released during nitrification are NO_3^-, and N_2O.[17] Catalysis of NO to NO_2^- occurs by O_2 oxidation in aerobic conditions[17] while an as yet unknown enzyme performs the conversion under anaerobic conditions. Nitrite oxidoreductase (NXR) performs the last step of nitrification.[18]

A host of stable isotope experiments have been performed in pure culture studies for nitrifying bacteria. In general, discrimination against the heavy isotope was seen when examining NH_4^+ oxidation to NO_2^- and conversion of NH_2OH to N_2O (Average $\eta = -29.6 \pm 4.9‰$, and $-56.6 \pm 7.3‰$, respectively).[3] Oxidation of NH_4^+ to N_2O also showed preferential incorporation of the light isotope, though weaker than either of the other two reactions (Average $\eta = -5.1 \pm 12.0‰$).[3] In contrast, NO_2^- transformation to NO_3^- revealed a preference for the heavy isotope (Average $\eta = -13.0 \pm 1.5‰$).[3]

Comammox combines the processes of AOA/B and NOB, enabling NH_3/NH_4^+ oxidation to NO_3^- to occur in a single organism. Discovered in 2015, relatively little is known about this process. Thus far, two bacterial species in the genus *Nitrospira* have been identified as comammox organisms, and it is known that the A subunit of the AMO in the comammox organisms is distinct from that of AOA/B AMO. The distinct AMO has enabled researchers to identify *Nitrospira* in forest soils, rice paddy soils, rice rhizospheres, and brackish lake water. Metagenomic studies suggest comammox organisms are even more widespread, with putative

Nitrospira species found in wastewater treatment plants, drinking water treatment systems, agricultural soils, and freshwater habitats.[19]

Finally, ammonia and ammonium can be processed by what is known as anammox. Rather than converting ammonia to NO_2^- or NO_3^-, the end product of anammox is N_2:[20]

$$NH_4^+ + NO_2^- \rightarrow N_2 + H_2O$$

Most of the research performed on anammox revolves around wastewater treatment, but anammox has been seen in natural settings as well, including freshwater environments, marine environments, and terrestrial environments.[21] Thus far, all bacteria capable of anammox are in the planctomycete phylum which contains aquatic bacteria. Planctomycetes are characterized by pits in the cell surface, no peptidoglycan in the cell walls, budding reproduction, and internal cell compartmentalization. As HAO has only been found inside a cytoplasmic membrane bound compartment, it has been proposed that there is an 'anammoxosome' in these bacteria.[21] Stable isotope tracing for anammox was reported by Brunner *et al.* who determined that the ^{14}N is preferentially incorporated into the product.[22] No stable isotope tracing for comammox has not yet been reported.

NO_3^- to NH_4^+/N_2O/N_2: DNRA, Denitrification, Nitrifier-denitrification, and Co-denitrification

NO_3^- in the soil has one of three ultimate fates: assimilatory nitrate reduction (plant uptake), conversion into ammonium by what is known as the dissimilatory nitrate reduction to ammonium (DRNA) pathway, or conversion into N_2O or N_2 in one of the many denitrification processes. In a biological context, DRNA and denitrification are simply different methods of utilizing nitrate for anaerobic respiration. Each process has its own advantage: the DRNA

pathway transfers more electrons than denitrification (eight as opposed to five per initial nitrate substrate), but denitrification is ubiquitous.[23,24]

DNRA is an anaerobic process in which microbes convert NO_3^- to NO_2^- to NH_4^+. Two types of DNRA are known, one paired to sulfur oxidation and the other coupled to fermentation.[23] Several different species of bacteria are capable of fermentative DNRA including *Pseudomonas spp., Clostridia, Vibrio spp.,* and *Desulfovibrio spp*. Environments that favor DNRA over denitrification are still being elucidated, but there is some evidence that DNRA prevails in highly reducing conditions with low nitrate availability and high organic matter.[25,26] No stable isotope studies have been performed at the time of writing this chapter.

The process that closes the nitrogen cycle and reduces NO_3^-/NO_2^- to N_2 is known as denitrification, and this process is performed under anaerobic conditions by denitrifying organisms. Some traditional nitrifiers have been found to be capable of denitrification as well, and to differentiate denitrification performed by nitrifiers and denitrifiers, denitrification by nitrifying microbes is termed nitrifier-denitrification.[27] Both pathways use the same four enzymes to transform nitrate to N_2, and these enzymes catalyze the following stepwise reactions:

$$NO_3^- + 2\ e^- + 2\ H^+ \rightarrow NO_2^- + H_2O$$

$$NO_2^- + e^- + 2\ H^+ \rightarrow NO + H_2O$$

$$2\ NO + 2\ e^- + 2\ H^+ \rightarrow N_2O + H_2O$$

$$N_2O + 2\ e^- + 2\ H^+ \rightarrow N_2 + H_2O$$

These reactions are carried out sequentially by nitrate reductase (Nar), nitrite reductase (Nir), nitric oxide reductase (Nor), and lastly, nitrous oxide reductase (Nos).[28] Archaea, yeast, fungi,

and bacteria are all capable of denitrification, though studies have mostly focused on fungal and bacterial denitrification.[27] Fungi are the predominant denitrifiers in grassland and woodland soils, while bacteria dominate in agricultural soils.[29,30]All known denitrifying fungi lack N_2O reductase, thus releasing N_2O as their final product.[30]

A process termed co-denitrification can occur simultaneously with denitrification. In co-denitrification, the co-substrates of denitrification are used to nitrosate an amino compound, resulting in N_2O or N_2 formation.[31,32] This is known to occur during fungal denitrification and particularly during catalysis of NO to N_2O by the fungal nitric oxide reductase, P450nor (discussed later).[31] Although the biological significance of this process is not fully understood, it has been proposed that co-denitrification acts as a nitrogen immobilizing process as the inorganic nitrogen is bound to the organic N compounds.[32]

Denitrification has been particularly well studied, with stable isotopes and isotopic enrichment factors known for each step in the process, albeit with more or less precision. NO_3^- to NO_2^- reduction has been examined via soil incubations, water samples, and both fungal and bacterial pure culture studies. The general trend across all these experiments for both bacteria and fungi is preferential incorporation of the light isotope (average $\eta = -31.3 \pm 6.1‰$).[3] Pure culture studies of reduction of NO_2^- to NO show a similar though weaker trend as nitrate reduction (average bacterial $\eta = -11.8 \pm 4.5‰$, average fungal $\eta = -15.1 \pm 7.0‰$).[3] Soil incubation and pure culture studies on the reduction of N_2O to N_2 saw preferential incorporation of the light isotope as well, though to a lesser degree (average $\eta = -4.1 \pm 6.8‰$).[3] The only study that examined the isotopic preference for NO → N_2O catalysis was a fungal enzymatic study, and they observed an overall discrimination against the light isotope (although the ε for one of the N atoms was $36.1 \pm 1.2‰$ while ε for the other N atom was -12.6 ± 3.0).[33]

The Importance of N_2O

One of the common intermediates in the nitrogen cycle is N_2O. N_2O is a potent greenhouse gas with a 100-year warming potential approximately 265 times greater than that of carbon dioxide.[1] Additionally, N_2O is currently the chief anthropogenic contributor to ozone depletion in the atmosphere. Approximately two thirds of the processes in the known terrestrial nitrogen cycle (nitrification, comammox, denitrification, nitrifier-denitrification, and co-denitrification) produce N_2O as either an obligate intermediate or side product. Moreover, the nitrogen fluxes through processes that can produce N_2O are high. One study examining nitrogen loss in large northeastern United States water sheds estimated that half of all N_r applied to agricultural soils in these watersheds was denitrified.[34] It is therefore crucial to understand the environmental conditions in which the different nitrogen cycling processes dominate.

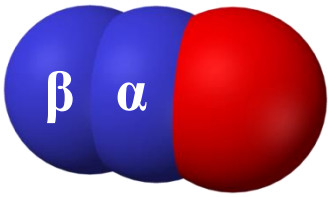

Figure 2. The atomic structure of nitrous oxide. The nitrogen atoms are in blue and the oxygen atom is in red. The α and β nitrogen atoms are labeled in the figure.

Here again, stable isotope studies have proven invaluable. The two nitrogen atoms in the asymmetric N_2O molecule are distinct, and the center nitrogen atom is termed the α nitrogen (N^{α}) and the terminal nitrogen atom is the β nitrogen (N^{β}, Figure 2). The difference in $\delta^{15}N$ between $^{\alpha}N$ and $^{\beta}N$ is known as site preference (S_P). S_P has been shown to be a robust indicator of the processes making N_2O because unlike bulk $\delta^{15}N$ measurements, S_P has been shown to be nearly

constant in pure bacterial cultures as a function of substrate concentration.[35,36,37] Moreover, S_P is different for different processes. The S_P for fungal denitrification is ~-37‰ in pure culture studies, which is similar to the S_P obtained from pure culture bacterial nitrification studies (S_P = ~33‰).[35,36] However, pure culture studies examining bacterial denitrification reveal an S_P value of approximately -10 to 0‰, making it distinct from bacterial nitrification and fungal denitrification.[35] Haslun et al. recently examined the effect of varied carbon source concentrations of two bacterial dentirifiers and showed that S_P remained consistent while growth rate and bulk $\delta^{15}N$ varied markedly.[37]

While identifying the microbial source of N_2O is a vital step toward mitigation, it is equally important to understand the enzymes involved in N_2O production. Approximately 80% of all anthropogenic N_2O produced is the result of agricultural fertilization practices, and both bacterial and fungal denitrification take place in agricultural fields.[29,38,39] Because both processes utilize NORs to produce N_2O, understanding the types and biochemical mechanisms of the different NORs will further our ability to identify N_2O production pathways as a means for reducing the emission of anthropogenically produced N_2O.

Nitric Oxide Reductases: Detoxifying NORs

A variety of NORs has been discovered with their physiological functions encompassing two categories: NO detoxification and/or anaerobic respiration.[31,40,41,42] Two known detoxifying NORs are FNOR (flavorubredoxin) and Hcp (hybrid cluster protein). A fairly recent discovery, flavorubredoxin (known as both FNOR and FIRd) belongs to the A-type flavoprotein family. Crystal structures show that FIRd consists of an N-terminal metallo-β-lactamase-like domain and a C-terminal flavodoxin domain. The diiron catalytic site is contained in the N-terminus while a

flavin mononucleotide (FMN) resides in the C-terminus.[43] Initial characterization revealed that FIRd is reduced by NADH:oxidoreductase (FIRd-red), which is encoded in the same gene locus as FIRd. Activity assays indicate that FIRd has a high specificity for NO, with turnover numbers similar to that of the more well-known cytochrome *c* NOR (cNOR, discussed later).[41] Studies to elucidate its mechanism are currently underway.[44]

Hybrid cluster proteins (Hcp) are soluble proteins known to contain a unique iron-sulfur-oxygen cluster ([4Fe-2O-2S]).[42] First proposed to be involved in nitrate/nitrite respiration, it has recently been demonstrated that, in *Escherichia coli* at least, Hcp is an NO detoxifying NOR. A combination of microbial gene deletion studies and purified enzyme studies demonstrated that Hcp is a high-affinity, low-capacity NOR that is expressed under ambient physiological conditions, while other NORs are expressed under high NO stress conditions. It is further known that Hcp is reduced by an NADH-dependent reductase, Hcr, which also serves to protect Hcp from inactivation by nitrosative damage during high NO concentrations.[42] As the function of Hcp has just been elucidated, a mechanism has not yet been proposed.

Respiratory NORs

Three types of respiratory bacterial NORs are known as well as one fungal respiratory NOR. The most well studied bacterial NOR is cNOR, which was first purified in 1989 from the bacterium *Pseudomonas stuzeri.*[45] cNOR is an integral membrane protein that consists of two subunits named NorC and NorB. NorC (17 kDa) is the smaller of the two, and contains a globular region with a low spin heme *c* that faces the periplasmic side of the membrane. NorC also has a single transmembrane helix which anchors it to the membrane. Functionally, NorC serves as the electron shuttle between cytochrome c_{550} and NorB, which is the catalytic unit. NorB (56 kDa) is

a membrane protein, containing 12 helices. A low-spin heme *b* in NorB passes electrons from NorC to the active site in NorB, which is a binuclear center (BNC) made of a high-spin heme *b*, called heme b_3, and a non-heme iron, termed $Fe_{B,}$ which are antiferromagnitically coupled to each other in the oxidized state.[46,47] cNOR is a member of the heme-copper oxidase (HCO) superfamily and structurally homologous to the cbb_3-type oxidases. All six ligand coordinating histidines found in HCOs are strictly conserved in cNOR, with the main differences between HCO and cNOR being the exchange of the Cu for an Fe at the active site and no proton translocation channels in cNOR. Due to the homology of the cNOR to cytochrome *c* oxidases, the cytochrome *c* oxidase nomenclature was adopted for NOR.[47]

cNOR was successfully crystalized from *Pseudomonas aeruginosa* in 2012 (Figure 3). New insights that were gained were the presence of a μ-oxo-bridge between the BNC in the resting state and a calcium binding site in NorB. The calcium is located between the propionates of heme *b* and b_3, and it is thought to possibly control electron transfer between heme *b* and heme *c* or to stabilize the interaction of NorC and NorB.[48]

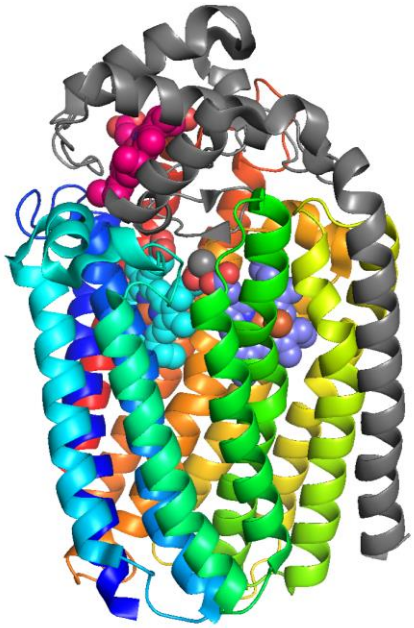

Figure 3. Crystal structure of cNOR from *Pseudomonas aeruginosa*. NorC is shown in grey with the heme *c* in pink. NorB, the catalytic subunit, is shown in rainbow with heme *b* (cyan heme), heme b_3 (purple heme), Fe_B (brown sphere) and the calcium ion (grey sphere). The figure was prepared with PyMol using PDB:3O0R.[49]

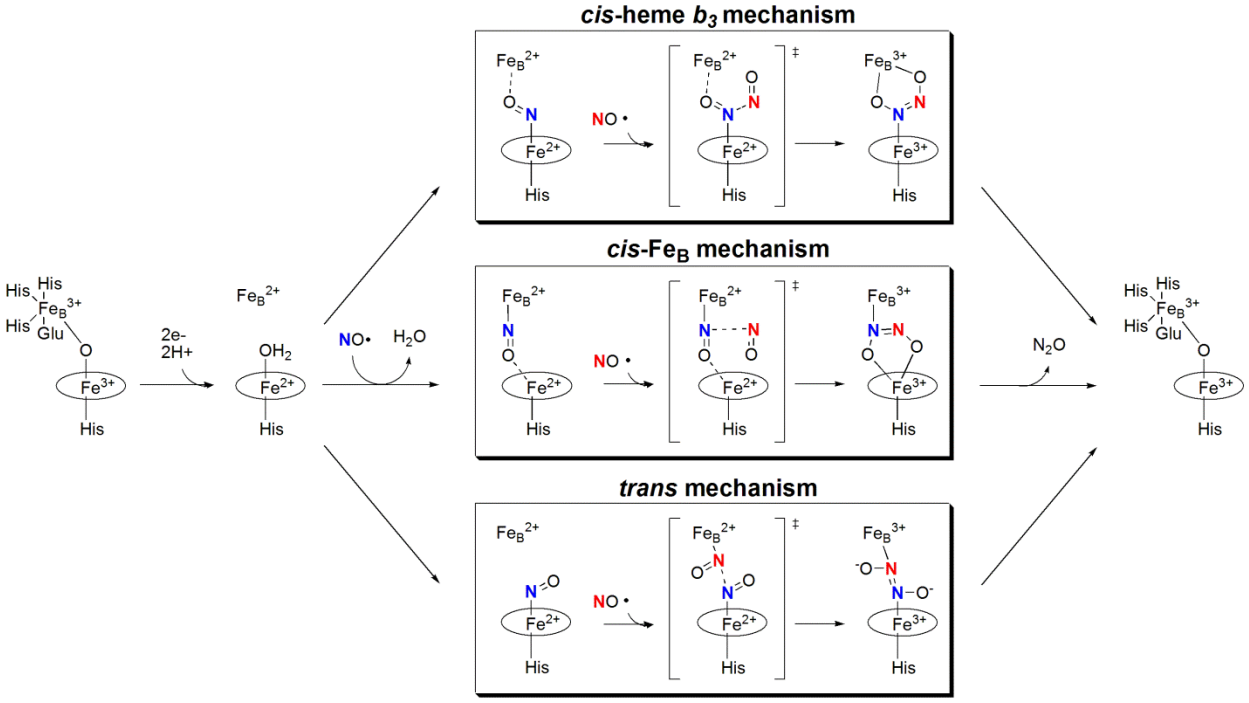

Figure 4. Three distinct proposed mechanisms of cNOR, adapted from Moënne-Loccoz.[50]

At present, three different mechanisms of N_2O production are proposed for cNOR (Figure 4). The first proposed mechanism is termed the *cis*-heme b_3 mechanism. This mechanism proposes that all catalysis occurs on the heme Fe, and the Fe_B helps to coordinate the NO and donate electrons. There is some experimental evidence for this mechanism in the form of membrane potential studies and optical spectroscopy,[51] but the greatest support comes from computational studies, which shows this mechanism contains the lowest energy barriers.[52]

The second mechanism is known as the *cis*-Fe_B mechanism, which is similar to the *cis*-heme b_3 mechanism but catalysis occurs on the Fe_B. Currently there are some kinetic studies and cyclic voltammetry data that are consistent with this mechanism.[53,54] While a mechanism involving a dinitrosyl iron complex on the Fe_B site has been ruled out,[55] it could be possible to have a mechanism in which the first NO molecule binds to the Fe_B and is then attacked by the second NO before forming the N-N bond (as shown in Figure 4).

The third mechanism is known as the *trans* mechanism, in which one NO molecule binds to each Fe in the BNC before N-N bond formation occurs. Structural studies, steady state kinetics, electron paramagnetic resonance (EPR), and resonance Raman studies support this mechanism.[48,56,57,58] This is also the mechanism proposed for a cNOR mimic, which has been well studied.[59,60,61]

A second type of bacterial respiratory NOR is known as qNOR, and this enzyme uses quinol as its biological reductant. Structurally, it is quite similar to cNOR, the major differences between the two being an extended N-terminus on qNOR and a water channel to the active site that is not

present in cNOR.[40,62] Due to its high similarity to cNOR, qNOR will not be discussed in extensive detail in this chapter.

The only NOR known to generate an electrochemical gradient was isolated from *Bacillus azotoformans* and is known as Cu_ANOR.[63] Though no crystal structures have been solved yet, homology modeling to cytochrome ba_3 from *Thermus thermophilus* predicts that Cu_ANOR consists of 12 transmembrane helices and has a di-copper site, one heme *b*, and a binuclear center that contains a heme b_3 and a non-heme iron. It is known that Cu_ANOR uses cytochrome c_{551} as a reductant, and is used in anaerobic respiration.[64] No mechanism has yet been proposed for this NOR, but given the high structural similarity of Cu_ANOR to cNOR, it is likely that the mechanism of the two NORs are similar.

In denitrifying fungi, one type of NOR has been discovered. Known as P450nor due to the P450 heme that serves as the catalytic site, P450nor catalyzes the reduction of NO to N_2O via:

$$NAD(P)H + H^+ + 2\ NO \rightarrow NAD(P)^+ + H_2O + N_2O$$

P450nor (~46 kDa) is a soluble protein consisting of a single subunit. It is encoded by a single gene (CYP55) and is found in both the cytoplasm and mitochondria.[31,65] Early research indicated that P450nor received electrons from NAD(P)H, but it was not until a crystal structure was solved that it was suggested that NAD(P)H directly reduced P450nor. The authors noted that the distal pocket of the heme was much more open to the solvent than P450 monooxygenases and could potentially be an NAD(P)H binding site.[65] Kinetic studies and additional crystal structures with NADH analogs confirmed direct reduction of P450nor by NAD(P)H. This is quite surprising given that all other P450s must be reduced one electron at a time.[31]

As the known fungal denitrifiers do not contain a Nos, they cannot catalyze the final step in denitrification and convert N_2O to N_2.[31] This is somewhat overcome by the process of co-denitrification in which nitrite and a second nitrogen donor (reduced relative to N_2) are combined by P450nor to form either N_2O or N_2. The final product is dependent on the redox state of the second nitrogen atom, with more oxidized species yielding N_2O and more reduced species yielding N_2.

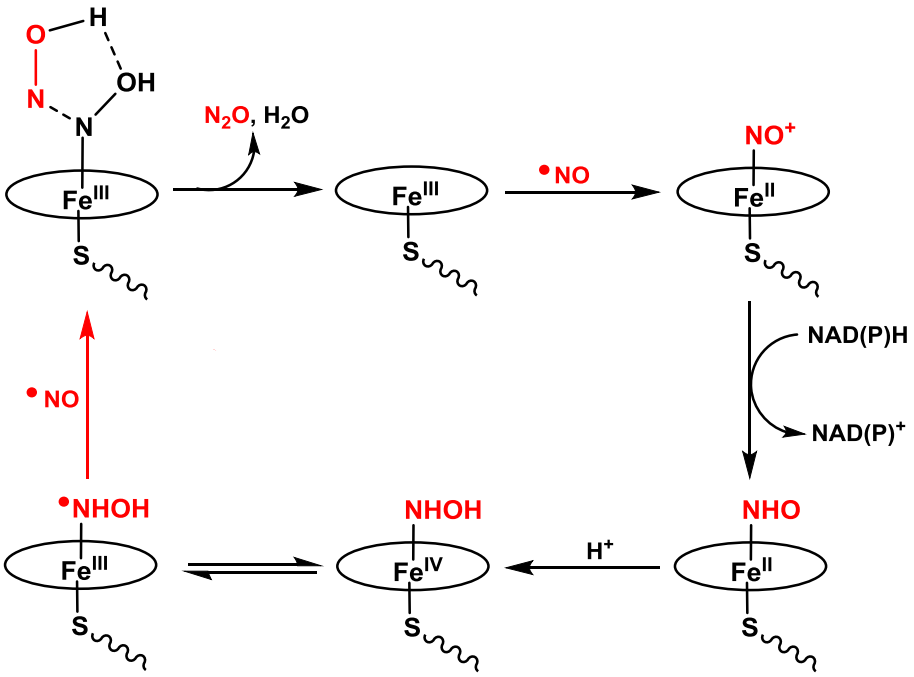

Figure 5. The proposed mechanism of P450nor. NO binds to the ferric heme, which is then reduced directly by NAD(P)H. The reduced intermediate is doubly protonated before the second NO attacks, forming what is proposed to be a cyclic intermediate. In the last step, the cyclic intermediate breaks apart to yield H_2O and N_2O.

The mechanism of P450nor (Figure 5) has been studied extensively, and while the general mechanism is known, details about some of the intermediates are still being elucidated. In brief, the general mechanism of P450nor consists of two phases. First, one molecule of NO binds to the ferric heme, and this complex is reduced directly by NAD(P)H. After reduction, both the N and O are protonated before the second NO molecule binds and N_2O and H_2O are formed.[66] Density functional theory (DFT) calculations have shed light on the redox states of the various intermediates. For example, the (FeNO) species that forms after the first NO binds to the heme is best characterized as Fe(II)-NO^+, while after reduction it resembles Fe(II)-NO^-.[66,67] The double protonation event promotes binding of the second NO molecule and formation of N_2O and H_2O,

though exact details of this last step are lacking. It has been proposed that a cyclic intermediate forms when the second NO binds, however experimental evidence for this complex is lacking.

Stable Isotopes as a mechanistic probe

In comparison with the P450nor, the mechanistic knowledge about cNOR is relatively limited, as evidenced by the three proposed mechanisms. As an integral membrane protein, cNOR is difficult to isolate and purify. Even when enough protein is purified, the signals from the three hemes make gathering and interpreting spectroscopic data a challenge, at times providing results that could support multiple mechanisms.[51] Stable isotopes are uniquely suited to probe enzymatic mechanisms and have been used for decades in such studies across multiple disciplines.[68,69] Stable isotopes have also been used to examine the mechanism of enzymes in the nitrogen cycle. Most relevant to this chapter is the study by Yang *et al.*, who used natural abundance isotopes of NO to examine the catalysis of NO to N_2O via purified P450nor from the fungus *Histoplasma capsulatum*. [33] This study revealed that the first NO to bind to P450nor becomes the β nitrogen in the final N_2O molecule while the α nitrogen and oxygen are derived from the second NO binding. Yang *et al*. reached this conclusion by analyzing the kinetic isotope effects (KIEs) for the reaction. A KIE is the reaction rate of the light isotope (k_L) over the reaction rate of the heavy isotope (k_H).

$$\mathrm{KIE} = k_{\mathrm{L}}/k_{\mathrm{H}} \tag{6}$$

$$\mathrm{KIE} = \frac{1}{\alpha} \tag{7}$$

In this definition, the KIE can be greater than one, one, or less than one. If the KIE is greater than one, this is referred to as a normal isotope effect, in which the light isotope reacts more quickly than the heavy isotope. When a KIE less than one is obtained, the reverse is true, and the heavy isotope reacts more quickly than the light isotope. If the KIE is equal to one, both isotopes react at the same rate.

Several factors determine the KIE:

$$\mathrm{KIE} = \mathrm{ZPE} \cdot \mathrm{EXC} \cdot \mathrm{MMI} \cdot \mathrm{TSDF} \tag{8}$$

These include the zero-point energy (ZPE), excited vibrational states (EXC), the mass moment of inertia (MMI), and the transition state decomposition frequency (TSDF). Each of these terms is discussed in more detail below.

Zero-Point Energy and the ZPE Approximation

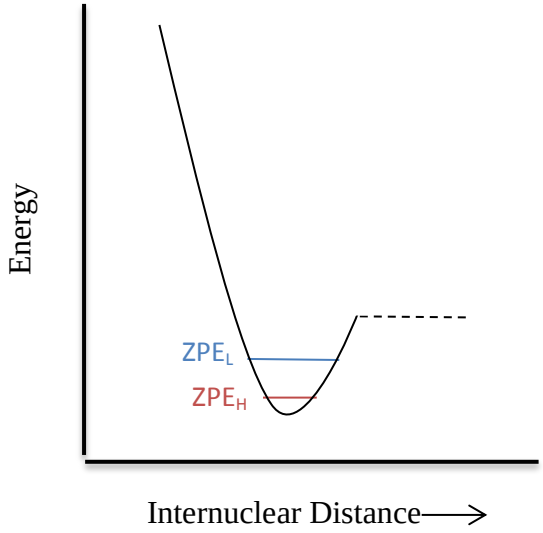

Figure 6. A diagram illustrating a bond as a harmonic quantum oscillator. As the atoms move from extremely close together (far left) to the point where the bond breaks (dashed line), the energy forms a well. In this well is the lowest energy state of the nucleus, termed the zero-point energy (ZPE). The ZPE for the lighter isotope (ZPE_L, blue line) is different than that of the heavier isotope (ZPE_H, red line) due to the differences in mass between the two isotopes.

In a simplified form, a bond between two atoms in the ground state can be thought of as a harmonic quantum oscillator. If energy is plotted as a function of internuclear distance, it can be seen that the energy decreases as the nuclei move further apart. After a certain point however, the energy begins increasing and eventually the bond connecting the nuclei is broken, resulting in a plateau (Figure 6) In the well that occurs in between these two extremes is a point where the nucleus is at its lowest energy level (i.e., the ground state). This lowest energy level is designated the zero-point energy. Due to quantum physics, it is possible to relate the zero-point energy to mass through the following equations:

$$E = {}^{1}/_{2}\, h\nu \qquad (9)$$

$$\nu = \frac{1}{2\pi c}\sqrt{\frac{k}{\mu}} \tag{10}$$

$$\mu = \frac{m_1 m_2}{m_1 + m_2} \tag{11}$$

where *h* is Planck's constant, ν is the frequency of the bond of interest, *c* is the speed of light, *k* is Boltzman's constant, μ is the reduced mass, and m_1 and m_2 are the masses of the atoms in the bond of interest. It can be seen that energy is proportional to the frequency of the bond, which is inversely proportional to the square root of the reduced mass of the atoms in the bond. Thus, if the mass changes (i.e., when one isotope is replaced with another), the energy will also change, yielding different ZPE's for different isotopes. A similar phenomenon is observed in the transition state, with different isotopes having different ZPE's.

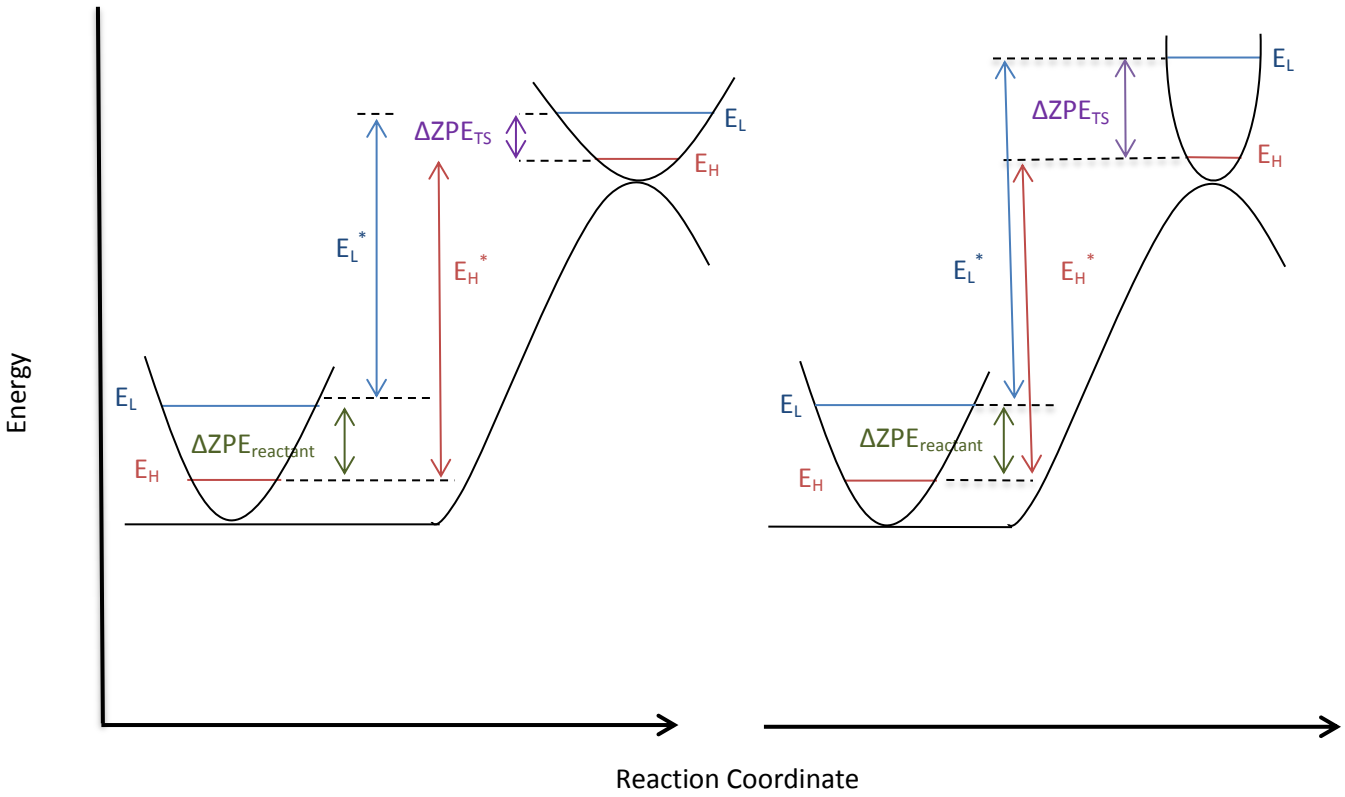

Figure 7. A diagram of a normal and inverse isotope effect. Energy is plotted against an arbitrary reaction coordinate. A normal isotope effect (in which the light isotope reacts more quickly than the heavier isotope) is shown on the left while an inverse isotope effect (where the heavier isotope reacts more quickly) is on the right. The red lines in the energy wells designate the ZPEs of the heavy isotope and the blue lines represent the light isotope ZPE. The difference in ZPE between the two isotopes is shown by the green arrow in the ground state and the purple arrow in the transition state ($\Delta ZPE_{reactant/TS}$). E_L^* and E_H^* stand for the activation energies of the light isotope and heavy isotope, respectively.

The wells in Figure 7 are Born-Oppenheimer electronic energy surfaces, which can be thought of as force fields. These force fields vary in steepness, which has implications for the nuclei of interest. If the well is shallow, then the force holding the two nuclei together is weak and the bond between them is "loose". If the well is steep, then the force holding the nuclei together is

strong and the bond is said to be "tight". The idea of tight versus loose bonds is important for determining the type of isotope effect that is observed and making mechanistic conclusions. For example, if the bond between the atoms of interest is looser in the TS than the ground state (Fig. 7, left panel), then a normal isotope effect is observed. In a normal isotope effect, the ZPE's of the light and heavy isotopes are close together in the TS. Because the lighter isotope has a higher ZPE in the ground state than the heavier isotope, the activation energy for the light isotope is lower than that of the heavy isotope. Thus, the light isotope reacts more quickly than the heavier isotope. Conversely, if the bond of interest is tighter in the TS than the ground state (Fig. 7, right panel), an inverse isotope effect occurs, and the heavy isotope reacts more quickly than the light isotope. This is because in the steeper energy well the TS ZPE's of the heavy and light isotopes are farther apart, which translates to a lower energy of activation for the heavier isotope.[70]

Over the course of many hydrogen/deuterium studies, it was noted that the ZPE was the largest single contributor to the observed KIE. As a result, the ZPE approximation was coined, which states that for all practical purposes, KIEs occur due to the differences in ZPE between the two isotopes of interest. While the ZPE approximation is valid for many H/D studies, it can begin to break down in certain circumstances, such as when examining heavier atom isotopes (like $^{14}N/^{15}N$). In this case, the other three terms in Equation 8 begin to contribute more substantially to the observed KIE.

Other contributors to the KIE

Excited vibrational states (EXC) accounts for the ability of different isotopes to populate the excited state levels of a bond. These levels are any of the energy levels above the ZPE. The

energy levels in a harmonic quantum oscillator are evenly spaced apart at $h\nu$, (Planck's constant times the frequency). Because bond frequency is directly related to bond strength, the excited state levels of bonds with higher frequencies are further apart. Above a certain vibrational frequency, however, the ambient energy provided by temperature is not sufficient to allow substantial occupation of these excited state levels. It has been demonstrated that EXC only significantly contributes to the KIE when the frequency (ν) of the bond of interest is less than 1500 cm^{-1}. Solving EXC mathematically for frequencies greater than 1500 cm^{-1} results in an answer very close to unity, thus highlighting that EXC does not greatly influence the final KIE in these instances.[71]

The mass moment of inertia (MMI) is the contribution to the isotope effect from the energy from translation and rotation of the molecule of interest. Previous experiments have shown that MMI begins to compete with ZPE as the prevailing contributor to the KIE under certain conditions. One case is when the molecules of interest are small enough that isotopic substitution could substantially change the mass and moment of inertia.[70]

The ZPE and EXC encompass the vibrational contributions to the KIE while the MMI is the contribution from the rotation and translation of the molecule. While the vibrational, rotational, and translational terms can be separated into different components, they are still ultimately related to one another. It is unsurprising, therefore, that changes in MMI result in changes in ZPE and EXC. For example, a study involving model calculations of secondary isotope effects (isotope effects occurring at a site other than the bond of interest) revealed that in some cases, changes in MMI were compensated by corresponding changes in ZPE and EXC.[70] In model studies of heavy atom KIEs, however, the compensation of EXC and ZPE was smaller, and MMI was the single largest contributor to the KIE. When MMI is the predominant driver of the KIE,

the final KIE can still be interpreted as a normal or inverse isotope effect, just as when the ZPE approximation holds. However, one can no longer use the ZPE approximation to explain the isotope effect. Additionally, calculating theoretical KIEs for reactions becomes more difficult due to the complicated interaction between MMI, ZPE, and EXC.[70]

The final contributor to the KIE is known as the TSDF. As the name implies, the TSDF is the tendency of the transition state complex to decompose into products. In theory, the TSDF contribution to the KIE can be calculated by hand if the correct parameters are known or can be approximated, as was demonstrated for hydrogen and deuterium in the theoretical reaction of a hydrogen transfer between two simple molecules.[72] With heavy atom isotopes, however, the calculations quickly become unwieldly and require advanced computational power to determine the TSDF.[70]

Summary

In this introduction, I have introduced the nitrogen cycle and reactions contained within the terrestrial portion of the nitrogen cycle. The different types of nitric oxide reductases were discussed with particular focus given to the two most well-studied NORs and the need for more mechanistic studies of cNOR. Uses of stable isotopes uses as both a tracer in the nitrogen cycle and a mechanistic probe were presented, and the quantum physical components that contribute to a KIE were discussed.

The remainder of this thesis will cover stable isotope mechanistic studies performed on purified cNOR from *Paracoccus denitrificans* (Chapter 2) and a cNOR mimic, I107EFe_BMb (Chapter 3). The isotopic studies on the native cNOR in Chapter 2 revealed that the enzyme did not discriminate between ^{14}N and ^{15}N in the α position of the N_2O molecule and discriminated

against the heavy isotope in the β position. For the cNOR mimic I107EFe_BMb in Chapter 3, N_2O production was observed, but the limited extent of reaction that was captured did not allow for KIE determination. Conclusions and future directions are presented in Chapter 4.

CHAPTER 2: Not so elementary: Isotopic fractionation and kinetic isotope effects of a purified bacterial nitric oxide reductase (NOR)

Clarisse M. Finders, Joshua A. Haslun, Hasand Gandhi, Peggy H. Ostrom, Nathaniel E. Ostrom, Eric L. Hegg

Joshua Haslun and Hasand Gandhi performed isotope ratio analysis of the N_2O molecules. Peggy Ostrom helped with data analysis and Nathaniel Ostrom and Eric Hegg helped with data analysis and guided the research.

ABSTRACT

Nitrous oxide (N_2O) is a serious concern due to its role in global warming and ozone destruction with a 100-year time horizon global warming potential approximately 265 times greater than that of carbon dioxide. Agricultural practices account for ~80% of all anthropogenic N_2O produced, due in large part to the stimulation of microbial denitrification as a result of over fertilization. To effectively mitigate N_2O emissions, it is vital to understand the microbial processes and enzymes responsible for N_2O production. Stable isotopes are uniquely suited to examine both microbial N_2O sources and the mechanism of N_2O biosynthesis through the use of site preference (S_P) and kinetic isotope effects (KIEs), respectively. Using trace gas isotope ratio mass spectrometry (TG-IRMS), we determined the $\delta^{15}N$, $\delta^{15}N^{\alpha}$, $\delta^{15}N^{\beta}$, and $\delta^{18}O$ for purified cytochrome *c* nitric oxide reductase (cNOR) from the model denitrifier *Paracoccus denitrificans*. We also calculated the

KIEs and associated isotopic enrichment factors (ε), and S_P ($S_P = \delta^{15}N^{\alpha} - \delta^{15}N^{\beta}$). Normal isotope effects were observed for bulk ^{15}N, $^{15}N^{\beta}$, and ^{18}O with average KIEs of: 0.0079 ± 0.0009 (average ε value of -7.8 ± 0.8‰), 1.0123 ± 0.0052 (Avg. ε = -12.2 ± 5.0‰), and 1.0180 ± 0.0008 (average ε = -17.7 ± 0.7‰), respectively. The isotope effect for the $^{15}N^{\alpha}$ was not statistically different from one (Avg. KIE=0.9993 ± 0.0023, Avg. ε = 0.7 ± 2.3‰,). S_P changed over the course of our reaction, ranging from ~9‰ to ~1‰. We present implications for the mechanism of N_2O production from cNOR based on our data as well as the main contributors to the observed KIE.

INTRODUCTION

Nitrogen is a key element to all life and exists as either reactive nitrogen species or dinitrogen gas (N_2). These two categories are connected to each other through an intricate cycle of pathways that includes nitrification, denitrification, anammox, comammox, dissimilatory nitrate reduction to ammonia (DNRA), and potentially others.[2,18] Nitrous oxide (N_2O) is one of the key intermediates in the nitrogen cycle. Unfortunately, N_2O is also a potent greenhouse gas, with a 100-year global warming potential approximately 265 times greater than that of carbon dioxide (CO_2), and is the largest anthropogenic source of ozone depletion.[73] Since the invention of the Haber-Bosch process, which fixes N_2 to ammonia, humans have had an enormous effect on both the amount and flux of bioavailable nitrogen, including N_2O. Currently, anthropogenic N_2O accounts for ~40% of all N_2O generated, with ~80% of this produced by microbial activity in response to agricultural practices.[38] With atmospheric N_2O concentrations increasing ~0.26% every year,[73] fully understanding the enzymatic processes that directly contribute to anthropogenic agricultural N_2O production is especially important.

Soil microbial processes that produce N_2O include nitrification, denitrification, and nitrifier-denitrification. Nitrification is the conversion of ammonium and ammonia (NH_4^+ and NH_3) to nitrate (NO_3^-) via hydroxylamine (NH_2OH) under aerobic conditions. During the oxidation of NH_2OH, N_2O is released as a side product. Denitrification and nitrifier-denitrification are processes that under anaerobic conditions convert NO_3^- to N_2 through a series of intermediates including nitric oxide (NO) and N_2O. Expanding our knowledge of enzymatic mechanisms of N_2O production is crucial to reducing anthropogenically produced N_2O.

Nitric oxide reductase (NOR), which produces N_2O from NO, is one of the most important enzymes in soil microbial N_2O production.[18] NOR activity can be found in both bacteria and fungi.[18,31] In its most generic form, NOR catalyzes the following reaction:

$$2\ NO + 2\ e^- + 2\ H^+ \rightarrow N_2O + H_2O$$

A single NOR occurs in fungi, consisting of one subunit (46 kDa). A P450-type heme serves as the catalytic center of the enzyme, giving P450nor its name.[65] Catalysis begins when an NO molecule binds to the ferric P450 heme, producing a heme-NO complex. The heme-NO complex is then reduced by NAD(P)H and doubly protonated, producing an intermediate that is best described as (Fe(III)-NHOH).[66] The final steps of the reaction that include binding of the second NO molecule followed by N_2O formation are less well understood.[31,67]

Thus far, four distinct bacterial NORs have been discovered, and several crystal structures have been documented.[43,42,62,74] Structural and sequence evidence show that quinol-dependent (qNOR) and cytochrome *c*-dependent (cNOR) NORs are evolutionarily related to the heme-copper oxidase family.[40] The most well studied bacterial NOR is cNOR, which is composed of two subunits, NorC (17 kDa) and NorB (56 kDa). NorC consists of one transmembrane helix, a

cytochrome *c* binding site, and a heme *c* which transfers electrons from cytochrome *c* to NorB. NorB is the catalytic unit and is an integral membrane protein with twelve transmembrane helices. Contained in the helices are two heme *b* molecules, termed heme *b* and heme b_3, analogous to the cytochrome *c* oxidase nomenclature.[75] Heme *b* receives electrons from NorC and passes them to heme b_3, which makes up half the catalytic site. The other half is a non-heme iron, termed Fe_B, coordinated to three histidines and a glutamate.[75]

Compared to our understanding of P450nor, our knowledge of the bacterial NOR mechanism is relatively limited. Three classes of mechanisms are currently proposed for cNOR, (Figure 8) mainly differing in where and how the NO molecules bind to the catalytic center. Two of the mechanisms propose that all of the chemistry occurs on one of the two Fe centers, with the first NO molecule binding to either the Fe_B iron (*cis*-Fe_B mechanism) or the heme (*cis*-heme b_3 mechanism) before being attacked by the second NO molecule.).[52,53] The third mechanism, known as the *trans* mechanism, suggests that one NO molecule binds to each iron.[58]

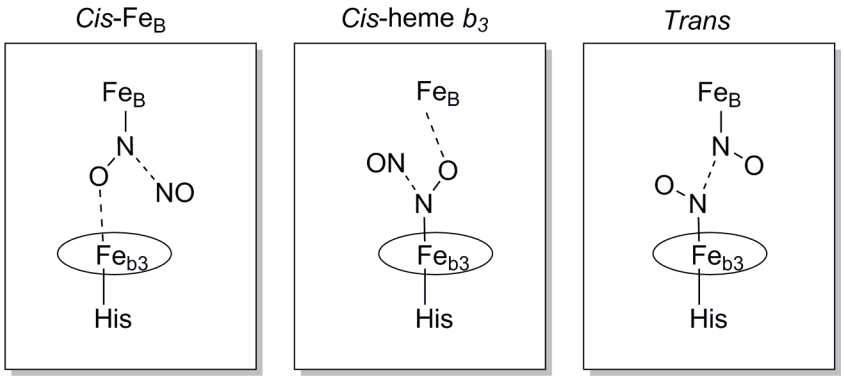

Figure 8. Three potential transition states during N_2O production by cNOR, adapted from Blomberg. [52] The catalytic site is a binuclear center that consists of the heme b_3 and a non-heme iron, Fe_B.

Stable isotopes have long been used to study enzymatic mechanisms through measuring kinetic isotope effects (KIEs). A KIE is defined as the rate constant of the light isotope divided by the rate constant of the heavy isotope. KIEs are useful in determining mechanisms and transition state structures because they provide a snapshot of the vibrational environment of the bonds of interest.[76] The two nitrogen atoms in the N_2O molecule are not equivalent, and therefore the center nitrogen (termed α) and the terminal nitrogen (termed β) will each have their own KIE, making stable isotopes particularly well-suited to investigate N_2O biosynthesis. In this context, we previously used stable isotopes to examine the production of N_2O by purified P450nor from *Histoplasma capsulatum*.[33] In this manuscript, we present the enrichment factors and KIEs for the $\delta^{15}N$, $\delta^{15}N^{\alpha}$, $\delta^{15}N^{\beta}$, and $\delta^{18}O$ of purified cNOR from the bacterium *Paracoccus denitrificans.* We also discuss energetic contributors to the KIE and mechanistic implications of our data.

MATERIALS AND METHODS

Materials

NO was purified by attaching a stainless steel trap (20 cm x 0.6 cm) and a 160 mL side-arm flask to a cylinder of 99.5% NO (Airgas) in a chemical fume hood. The molecular sieves (5A, 8 x 12 mesh; Arcos Organics) in both the trap and the flask were activated by heating the system to 180 °C under vacuum (~10^{-2} Torr) for 24 h. After cooling to room temperature, NO was allowed to enter the evacuated flask after passing through the molecular sieve trap.

All reagents were purchased from Sigma-Aldrich unless otherwise noted and used without further purification. Purified *P. denitrificans* cNOR was generously provided by Professor Pia Ädelroth.[77]

Enzymatic Assays: The cNOR activity assay (12.8 mL) was prepared by mixing 50 mM anaerobic 4-(2-hydroxyethyl)-1-piperazineethanesulfonic acid (HEPES) buffer (pH 7.5), 50 mM KCl, 0.5 mM *N,N,N′,N′* - tetramethyl-*p*-phenylenediamine (TMPD, Arcos Organics), 3 mM ascorbic acid, 20 μM equine heart cytochrome *c*, and 0.04% *n*-dodecyl-β-D-maltoside (DDM, Anatrace) in a 160 mL glass serum bottle in an anaerobic chamber (Coy). After the serum bottle was capped with a butyl stopper (Geo-Microbial Technologies, Inc.) and crimped, NO gas (10.3 μmols) was injected into the headspace of the serum bottle (147.2 mL) using a gas-tight syringe (Hamilton) and allowed to equilibrate for 15 min while shaking at 100 rpm at room temperature on a benchtop shaker (Thermo Scientific). To avoid potential diffusion of N_2O out of the reaction vial, the serum bottle was inverted before the cNOR (20 μL, 78 nM final concentration) was injected to initiate the reaction. The bottle was continuously shaken at 100 rpm during the course of the reaction. Prior to sampling, a volume of N_2 gas equivalent to the intended sample was injected to maintain a constant pressure upon sampling. The gas sample was then injected into a 30 mL sealed serum bottle that had been sparged with Ultra High Purity N_2. To ensure the enzyme was producing N_2O at the expected rate, one replicate was analyzed via gas chromatography (GC) on a Shimadzu Greenhouse Gas Analyzer, model GC-2014 (Columbia, MD), equipped with a Haysep N separation column and an electron capture detector (ECD). The conditions used were: 5% CH_4/95% Ar make up gas (Airgas) with a flowrate = 2.5 mL/min; N_2 carrier gas with a flowrate = 25 mL/min; 100°C GC oven temperature; 350°C ECD temperature. To obtain the isotopic composition of the N_2O produced, samples were analyzed on an IsoPrime 100 stable isotope ratio mass spectrometer (IRMS) interfaced to a TraceGas inlet system (Elementar; Mt. Laurel, NJ) as previously described.[33] Sample reproducibility (1 standard deviation) based on N_2O isotopic analysis of standards was 0.5, 0.5, 0.7, 0.7 and 1.2‰ for $\delta^{15}N$,

$\delta^{18}O$, $\delta^{15}N^{\alpha}$, $\delta^{15}N^{\beta}$, and S_P, respectively. The $\delta^{18}O$, $\delta^{15}N$, $\delta^{15}N^{\alpha}$, and $\delta^{15}N^{\beta}$ values of the laboratory pure N_2O standard were 40.15, -0.72, 10.19, and-11.65‰, respectively.

Two different sets of experiments were performed. The first set was performed to determine the isotopic enrichment factor for N_2O production by cNOR. Three replicates were sampled every forty min until enzymatic N_2O production began to plateau (~240 min). To determine if isotopic exchange between the water and NO was occurring, a second set of experiments was performed. Three replicates that spanned at least 10% of reaction completion were assayed, two of which were spiked with ^{18}O enriched water (87‰). Samples were taken every thirty min for 180 min. A control to test for the abiotic production of N_2O was prepared that included all reagents except the cNOR enzyme. N_2O above background was not detected via GC-ECD analysis under our reaction conditions, indicating that the N_2O observed in the first set of experiments was enzymatically produced.

Isotope nomenclature

The isotopic ratio R is defined as the abundance of the rare isotope over the abundance of the more abundant isotope:

$$R = \frac{\text{Heavy Isotope}}{\text{Light Isotope}} = \left(\text{i. e. } \frac{^{15}N}{^{14}N}\right) \quad (1)$$

Isotope values are expressed using the delta (δ) notation:

$$\delta = \left(\left(\frac{R_{sample}}{R_{standard}}\right) - 1\right) * 1000 \quad (2)$$

The international standards for $\delta^{18}O$ and $\delta^{15}N$ are Vienna Standard Mean Ocean Water and atmospheric N_2, respectively.[5] Mass overlap corrections (e.g., due to the presence of $N_2{}^{17}O$) were performed following the procedure of Toyoda and Yoshida.[78]

KIE and ε

For a closed system with an irreversible reaction, which describes our reaction conditions for the reduction of NO to N_2O, isotopic fractionation can be modeled using Mariotti's approximation of the Rayleigh equation:[7]

$$\delta_{\text{product}} = \delta_{\text{sample}} - \varepsilon_{\frac{P}{S}}\left(\frac{f*\ln f}{1-f}\right) \quad (5)$$

where *f* is the fraction of the substrate (NO) remaining, and the slope, ε, is the isotopic enrichment factor (a measure of the relative rates of the heavy and light isotopes). Once ε is obtained, the kinetic isotope effect (KIE), the ratio of the reaction rate of the light over the heavy isotopically substituted compounds, can be calculated from the following equations:

$$\varepsilon = (\alpha - 1) * 1000 \quad (6)$$

$$\text{KIE} = \frac{1}{\alpha} \quad (7)$$

$$\text{KIE} = k_L/k_H \quad (8)$$

where α is defined as the fractionation factor and k_L and k_H are the rate constants for the light and heavy isotopes, respectively. If the Rayleigh equation (Eq. 5) is plotted with the y-axis as the isotopic composition of N_2O at any point in time and the x-axis as *f**ln*f*/ (1-*f*), the slope is equivalent to isotopic enrichment factor (ε). In this relationship, the reaction begins at 1 on the right side of the graph (all substrate) and ends at 0 (no substrate remaining) on the left. To make

the data presentation more intuitive, all graphs presented in this manuscript use a close approximation of f*ln$f$/(1-f) for the x-axis, (1-f), in which reaction progress proceeds from left to right. All calculations of fitting, however, employ the full Rayleigh equation (Eqn. 5) as described above.

Statistics and Figures

To distinguish outliers in the data, the Grubb's test was used. This test identifies the presence of outliers based on the sample mean. Data obtained prior to a 1-f value of 0.1 were not included in the analysis to grant sufficient time for the reaction mixture to equilibrate and reach steady state. Least squares regression (LSR) was initially applied. However, because LSR is sensitive to influence by outliers, we applied Robust Linear Modeling (RLM) to determine the underlying trends in the data.[79] Results between the two approaches were compared and RLM decreased the standard error of the model without affecting the estimated parameters. All statistics were performed in the statistical software package R (R Foundation, version 3.4.1).

RESULTS

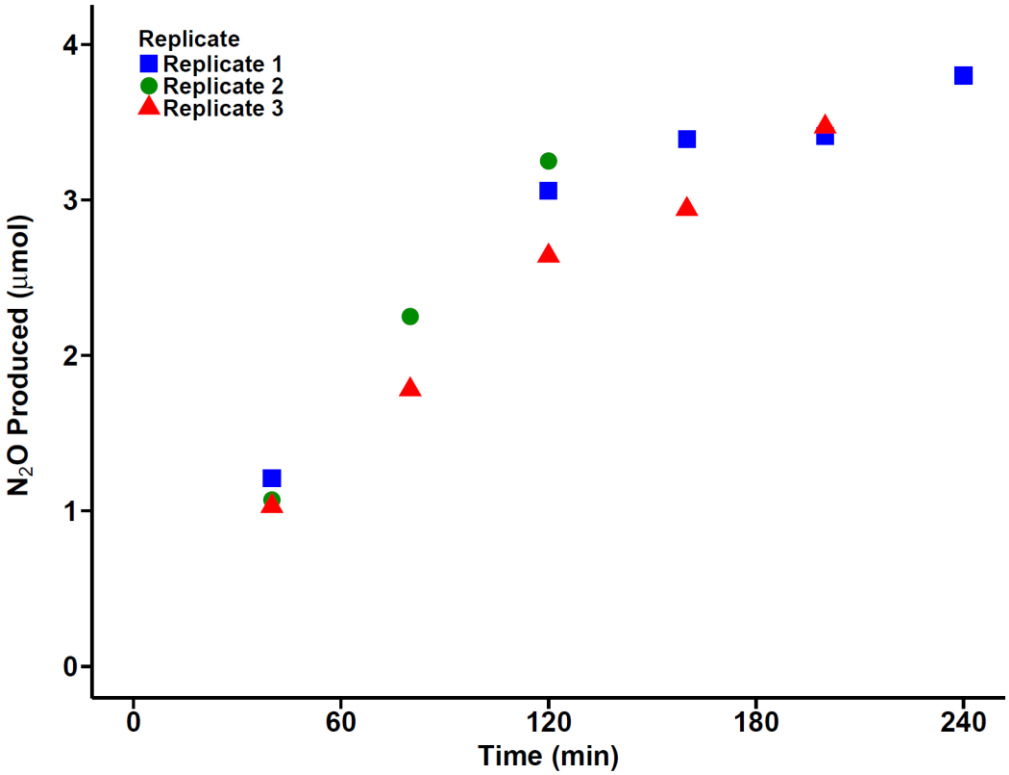

Figure 9. **Production of N_2O by *P. denitrificans* cNOR.** Each replicate contained 78 of cNOR and 10.3 µmols of NO gas, and the maximum amount of N_2O that could be produced was therefore 5.15 µmols. Three biological replicates were assayed.

Enzymatic N_2O Production

The production of N_2O by cNOR was monitored via GC-ECD over the course of 240 minutes. The rate of N_2O production averaged18 ± 7 nmol/min over the 180 min reaction (Fig. 9). Sufficient N_2O was produced over this time period to allow analysis by isotope ratio mass spectrometry.

Assessment of $\delta^{18}O$ and $\delta^{15}N$ of N_2O Produced by *P. denitrificans* cNOR

Isotope values ($\delta^{15}N$, $\delta^{15}N^{\alpha}$, $\delta^{15}N^{\beta}$, $\delta^{18}O$, and S_P) for the reduction of NO to N_2O by cNOR were measured over a range of ~20%-74% substrate conversion to product. Enzymatic activity began to plateau between approximately 3.2 and 3.8 μmol of N_2O produced (62-74% conversion, Figure S1). It is important to note that all KIEs presented in the manuscript are observed KIEs (KIE_{obs}) as opposed to intrinsic KIEs (KIE_{int}), which are defined as the inherent isotope effect for a specific step in a reaction.[80] Because the KIE_{int} can be partially masked by other steps in the reaction sequence, the observed KIEs should therefore be considered the lower limits of the intrinsic KIEs.[81]

A change of 9‰ in $\delta^{18}O$ was observed and application of the Rayleigh model (Eq. 5) yielded an average ε value of -17.7 ± 0.7 for the three replicates (Figure 10A, p-value ≤ 0.05, $R^2 \geq 0.95$). The positive slopes indicate a normal isotope effect in which the ^{16}O isotope reacts more rapidly than the ^{18}O isotope. This leads to an enrichment of ^{18}O in the residual substrate pool because ^{16}O is incorporated into the product more quickly. As the reaction proceeds, both substrate and product become more enriched in the heavy isotope over time, yielding a positive ε and a KIE > 1 (Table 1). The average KIE across all three samples was 1.0180 ± 0.0008,

An experiment was also performed with water enriched in ^{18}O to examine the possibility of isotopic exchange of oxygen between water and NO (Fig. 14-18). If exchange occurred, there would be a difference in the slopes of the isotopically enriched and unenriched replicates, with the slope of the ^{18}O enriched sample tending toward zero. As evident in Fig. S3A, there does not appear to be a difference between the ^{18}O spiked and non-spiked replicates, suggesting that if any isotopic exchange of oxygen occurred under our reaction conditions, it was below our detection

limit and could therefore be ignored. Although the *f* range of this control experiment was too small to accurately measure ε (Table 2), the general increase in $\delta^{18}O$ as the reaction progressed is further indication of a normal isotope effect for ^{18}O during N_2O production.

The $\delta^{15}N$ of N_2O has an ε value of -7.8 ± 0.8 with an increase in $\delta^{15}N$ slightly less than 4‰ over the measured reaction (Figure 10B, p-value ≤ 0.05, $R^2 \geq 0.8$). The average $\delta^{15}N$ KIE of the three samples was 1.0079 ± 0.0009, indicating that the reaction rate for ^{14}NO is faster than ^{15}NO.

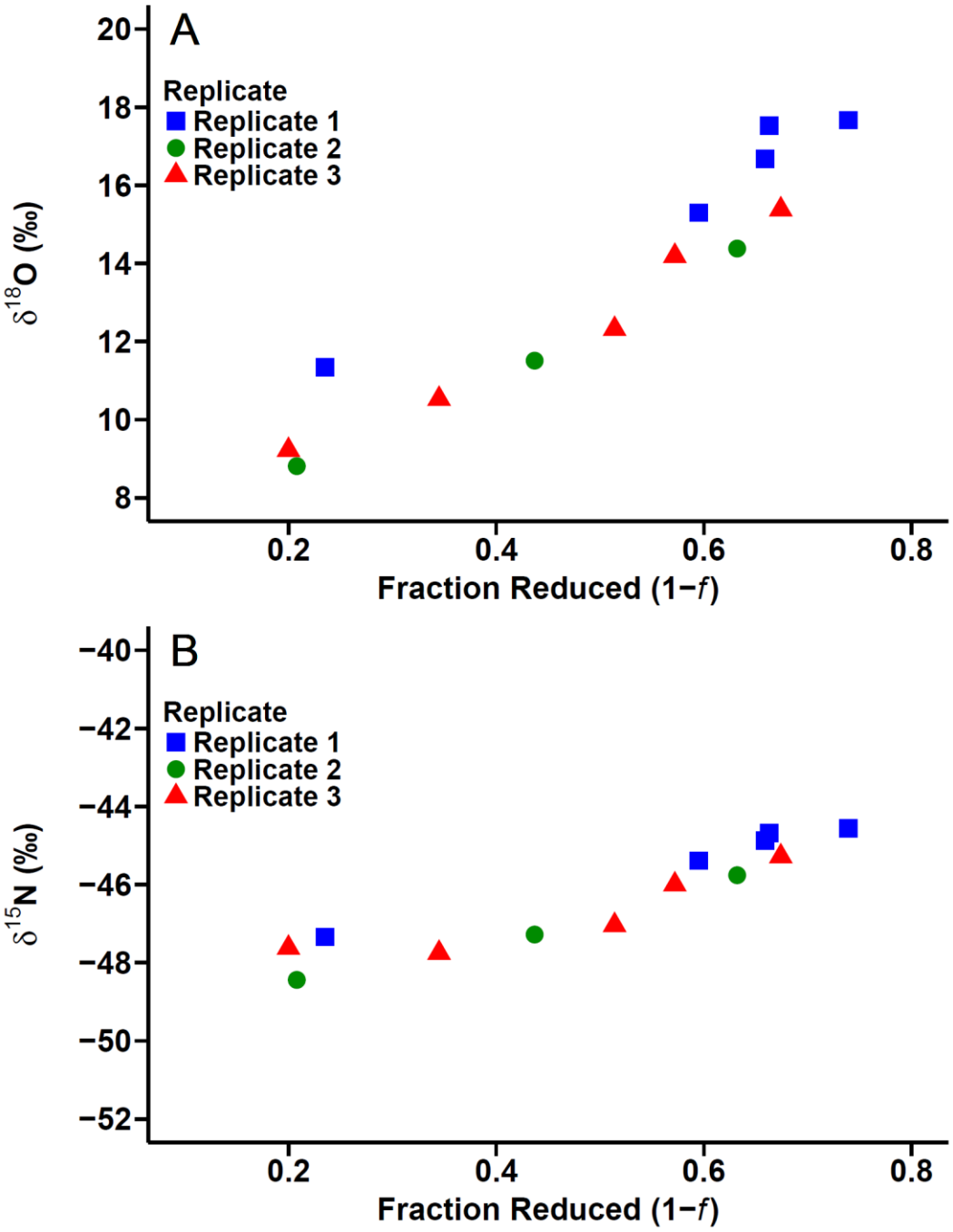

Figure 10. $\delta^{18}O$ (A) and $\delta^{15}N$ (B) of N_2O produced by cNOR as a function of the fraction of substrate (NO) reduced (1-*f*) with reactions progressing from left to right. Three biological replicates were assayed. The discontinuity between the 0.2 and 0.6 range of Replicate 1 resulted from a plugged needle during sampling.

Table 1. Isotopic enrichment factors (ε), p-values, R^2 values, and kinetic isotope effects (KIEs) of *P. denitrificans* cNOR.

Measurement	Replicate	ε	p-value	R^2	KIE
^{15}N	1	-7.6	0.0014	0.971	1.0077
	2	-8.8	0.0366	0.993	1.0089
	3	-7.1	0.0242	0.809	1.0072
	Avg ± SD	-7.8 ± 0.8			1.0079 ± 0.0009
$^{15}N^{\alpha}$	1	3.0	0.4298[a]	-0.045[a]	0.9971
	2	0.8	0.8327[a]	-0.865[a]	0.9992
	3	-1.6	0.3987[a]	-0.009[a]	1.0016
	Avg ± SD	0.7 ± 2.3			0.9993 ± 0.0023
$^{15}N^{\beta}$	1	-17.8	0.0172	0.847	1.0181
	2	-10.6	0.0013	1.000	1.0107
	3	-8.1	0.0697	0.625	1.0082
	Avg ± SD	-12.2 ± 5.0			1.0123 ± 0.0052
^{18}O	1	-16.8	0.0027	0.954	1.0171
	2	-18.2	0.0015	1.000	1.0186
	3	-18.00	0.0014	0.971	1.0183
	Avg ± SD	-17.7 ± 0.7			1.0180 ± 0.0008
S_P	1	-20.7	0.0563	0.672	0.9797
	2	-11.4	0.1572	0.881	0.9887
	3	-6.4	0.0345	0.750	0.9936
	Avg ± SD	-12.9 ± 7.3			0.9873 ± 0.0071

[a]The p-values and R^2 coefficients for N^{α} are largely meaningless because the N^{α} isotopic enrichment factors (ε) are relatively close to zero.

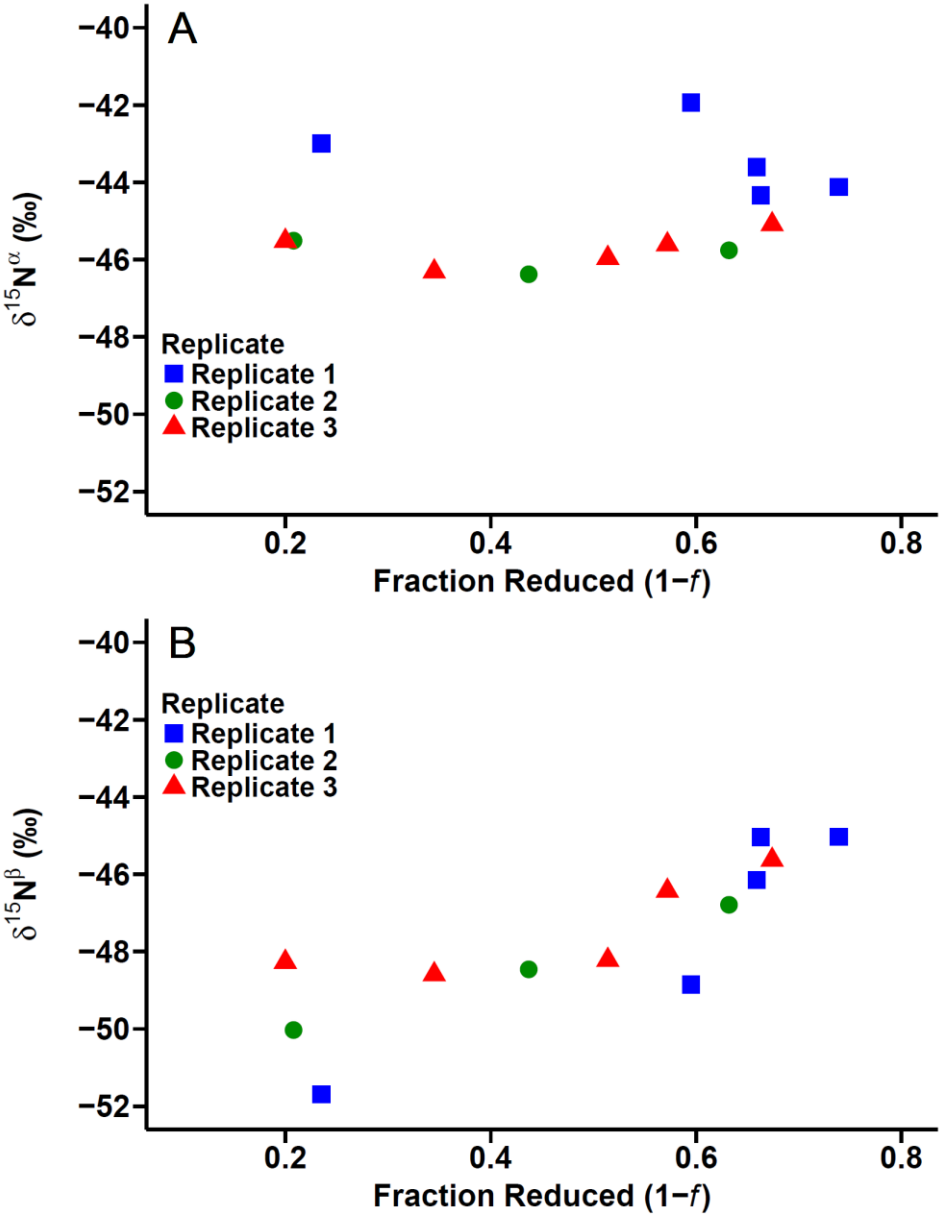

Figure 11. $\delta^{18}N^{\alpha}$ (A) and $\delta^{15}N^{\beta}$ (B) of N_2O produced by cNOR as a function of the fraction of substrate (NO) reduced (1-*f*) with reactions progressing from left to right. Three biological replicates were assayed.

$\delta^{15}N^{\alpha}$, $\delta^{15}N^{\beta}$, and S_P Values for N_2O Produced by *P. denitrificans* cNOR

The $\delta^{15}N^{\alpha}$ values remained essentially constant over the course of the reaction (Fig. 3A, p = 0.39 to 0.83), yielding a KIE of 0.9993 ± 0.0023, indicating that there is no significant discrimination

against ^{15}N by cNOR. While the enrichment factor (average $\varepsilon = 0.7$, Table 1) may indicate a real change, the standard deviation of 2.3 does not allow us to conclude that the slope is different than zero.

The absence of a KIE for $\delta^{15}N^{\alpha}$ indicates that the KIE observed for the $\delta^{15}N$ is driven by fractionation at the β position. $\delta^{15}N^{\beta}$ exhibited a range of 7‰ and an ε value of -12.2 ± 5.0 (Figure 11B). A normal KIE of 1.0123 ± 0.0052 was calculated using all three replicates (Table 1), indicating that ^{14}N is incorporated into the β position more rapidly than ^{15}N ($p = 0.0013$ to 0.0697). The control experiment with $H_2{}^{18}O$ indicated the same isotopic trends for the $\delta^{15}N^{\alpha}$ and $\delta^{15}N^{\beta}$ as discussed above (Figures 16A and 16B).

From *in vivo* studies of N_2O production, S_P has been found to be nearly constant over time, making it a valuable tool for distinguishing N_2O derived from nitrification versus denitrification.[6,82] In the current study, we have a closed system with a finite pool of substrate. We would therefore expect S_P to change over the course of the reaction as substrate is depleted if the α and β positions in N_2O experience unique KIE's. Although the slopes of the replicates differ, (Table 1) an overall trend of decreasing S_P during the course of the reaction can be seen (Figure 12).

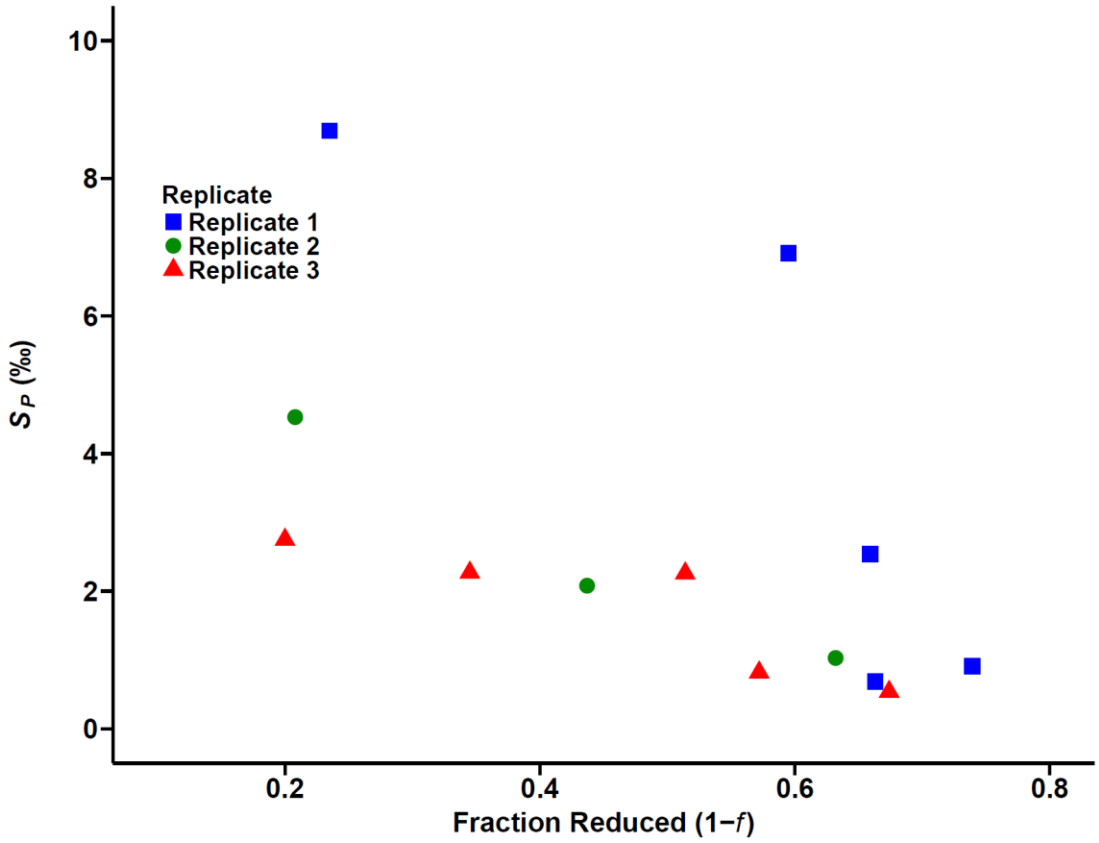

Figure 12. S_P ($S_P = \delta^{15}N^{\alpha}-\delta^{15}N^{\beta}$) for cNOR over the course of the enzymatic reaction. S_P is plotted against the fraction of substrate (NO) reduced with the reaction progressing from left to right. Three biological replicates were assayed.

DISCUSSION

Considerations of Observed KIEs

In this manuscript, we measured the observed KIEs for the N^{α}, N^{β}, and ^{18}O to gain mechanistic insights into cNOR from *P. denitrificans.* As previously mentioned, these are observed KIEs and should be taken as the lower limit of the intrinsic KIEs for the isotopically sensitive steps in the reaction. Any slight variation in enzymatic assay conditions could affect the rate of individual steps in the reaction sequence. This could, in turn, alter the extent to which the intrinsic KIEs are expressed.[80] leading to variation in both the ε values and the observed KIEs.

It is also important to note that other reactions could influence the isotope ratio of the enzymatically-produced N_2O. One such reaction is the exchange of oxygen between water and NO. Results from monoculture experiments led Kool *et al*. to propose that exchange of oxygen occurs during either the reduction of nitrite (NO_2^-) to NO or the conversion of NO to N_2O.[83] The lack of oxygen exchange observed in our experiments implies that any exchange must occur before conversion of NO to N_2O. Furthermore, as the reduction of $NO_2^- \rightarrow$ NO yields the smallest energy gain of the entire denitrification process, it can be argued that this is the most likely step to be reversed and therefore allows for a greater chance for oxygen exchange.[83]

Other reactions to consider are any processes that consume or produce NO or N_2O. There is no indication in the current literature that cNOR can reverse N_2O formation (i.e., oxidize N_2O to NO). At pH 7.0, the standard reduction potential of NO $\rightarrow$ N_2O at pH 7 is + 1.18 V, indicating that this reaction is highly exergonic and unlikely to be easily reversed.[84] In addition, there is currently no evidence that cNOR can further reduce N_2O to N_2. Another way N_2O could be produced is via co-denitrification, a process in which inorganic nitrogen (NO_3^- or NO_2^-) reacts with an organic source, such as an amino acid.[85] Due to the reducing conditions of our reaction and the sources of nitrogen available (NO, TMPD, and the buffer), it is highly unlikely that co-denitrification is taking place. Finally, control experiments in the absence of cNOR did not produce any detectable N_2O.

Insights from Site Preference

Previous bacterial culture studies examining N_2O production during denitrification demonstrated that S_P values remained essentially constant .[35,37] One explanation for this observation could be that the KIE's for both the α and β N in N_2O are the same. If this were the case, the difference

between N^{α} and N^{β} would remain constant during the course of the reaction, resulting in an unvarying S_P. However, the large range in ε for S_P (ε= -6.4 to -20.7‰) in this manuscript presents clear evidence that the KIEs for the α and β N atoms are not identical. This change in ε is consistent with our previous *in vitro* study of P450nor.[33] As a result, S_P fractionates over the course of the enzymatic reaction, and it has the potential to do so within cells as well. An alternative explanation for the consistent S_P observed during bacterial denitrification is that *f* is being held constant in the cell,[33,37] which could occur if the rate of NO production is approximately equal to its reduction to N_2O. The lack of expression of the enzymatic fractionation within bacterial cultures implies that NO is effectively held at steady-state levels within cells. It should be noted that an S_P value of 5.9‰ for purified *P. denitrificans* cNOR has been reported by Yamazaki *et al.*[86] This measurement is the result of data taken at a single time point in the reaction rather than over the course of the reaction. Thus, Yamazaki's S_P value and the S_P data presented here for cNOR cannot be directly compared.

Mechanisms and Mechanistic insights

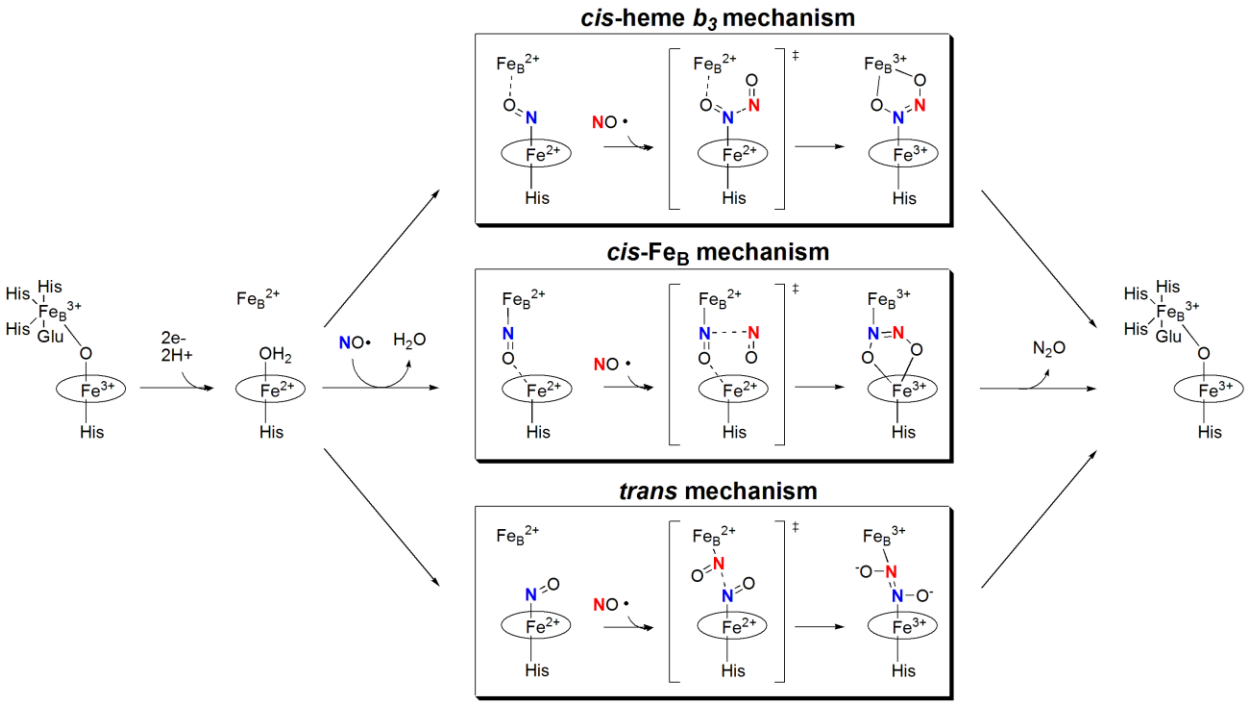

Figure 13. Three distinct proposed mechanisms of cNOR, adapted from Moënne-Loccoz.[35]

Currently there are three distinct mechanisms proposed for cNOR (Figure 13), all with varying levels of evidence. One mechanism is the *cis*-heme b_3 mechanism, in which the majority of the chemistry is proposed to occur at the heme iron.[87] In this mechanism, the first NO enters the catalytic site and binds to the reduced ferrous heme. The second NO then directly attacks the first NO to form the N-N bond. From here, it is possible that a cyclic intermediate forms which breaks apart to yield N_2O. Optical spectroscopy and membrane potential studies by Hendriks *et al.*[88] support this mechanism. This mechanism was also calculated to be the most energetically favorable by Blomberg, who compared all three different mechanisms.[52] A second mechanism is

the *cis*-Fe_B mechanism, which is identical to the *cis*-heme b_3 mechanism except that the reaction occurs on the non-heme iron. Steady-state kinetic studies[53] and cyclic voltammetry[54] data are consistent with this mechanism. In the *trans* mechanism, one NO binds to each iron, and the NO molecules then combine to form the N-N bond. This mechanism is supported by a large amount of experimental data, including steady state kinetics, EPR studies, and structural studies.[56,58,75] Additional evidence comes from a cNOR mimic, engineered by the Lu lab.[89] Lin *et al.* not only confirmed N_2O production by this engineered enzyme,[59] they also provided evidence that catalysis proceeded through a *trans* mechanism.[61] It is worth remembering, however, that this mimic could utilize a different mechanism than the natural enzyme.

For several decades, KIEs have been used as a probe for enzymatic mechanisms.[90,69] To draw mechanistic information from KIEs, hypothetical bond order and bond distances in the transition states must be determined. An example may be seen in our previous work on the P450nor from *H. capsulatum*, in which the first NO binding event to the enzyme was examined.[33] When considering the mechanism of cNOR, it is important to realize that there are at least two different steps that could affect the observed KIE; one when the first NO binds to an Fe, and the second when the N-N bond forms. At present, there is very little data available for either bond length or order in the transition states of these two states. Blomberg calculated 2.07 Å for the N-N bond distance during the second transition state in the *cis*-heme b_3 mechanism.[52] As this is a very long and weak bond, one would not expect to observe an isotope effect for this step because the bond order for NO has essentially not changed. This could be consistent with our observed N^{α} data.

Berto *et al.* combined spectroscopy and DFT calculations to study a model of the Fe_B site.[91] Adding NO to the reduced Fe(II) form of the models resulted in the formation of an Fe(III)-NO^- complex, with an electron moving to a largely NO antibonding orbital and a concomitant

lengthening of the NO bond. Additionally, changing the coordinating ligand on the model resulted in a range of N-O stretching frequencies, indicating that it is possible to tune the properties of the {FeNO} species by altering the extent of π back-bonding between the Fe and NO.[91] If cNOR behaves similarly to these models, a normal isotope effect would be expected for either *cis* mechanism, with the magnitude of the effect depending on the extent of π back-bonding between the NO and the Fe. The small normal isotope effect observed for N^{β} could be consistent with this sort of binding event.

Contributions to KIE

The zero-point energy (ZPE) approximation has been used to explain the cause of KIEs on a physical level. The ZPE is the lowest energy level occupied by a nucleus, and the ZPE approximation states that isotope effects are due to differences in ZPE between bonds comprised of the lighter and heavier isotopes in both the reactant state and transition state (TS). In addition to ZPE, however, three other energetic components exist that also contribute to the observed KIE. These components are: (1) excited vibrational states (EXC), which account for the ability of the different isotopes of interest to populate the excited vibrational states, (2) mass-moments of inertia (MMI), which is the contribution to the isotope effect from the energy from translation and rotation, and (3) the transition state decomposition frequency (TSDF), the probability of the transition state complex to decompose into products rather than reverting to reactants. Thus, in mathematical form, a KIE as defined by Bigeleisen and Wolfsberg is:

$$\mathrm{KIE} = \mathrm{ZPE} \cdot \mathrm{EXC} \cdot \mathrm{TSDF} \cdot \mathrm{MMI} \qquad (9)$$

The ZPE approximation has been used to explain KIEs in many H/D studies where the difference in ZPE between the two isotopes is great. In heavy-atom isotope effects, however, the energy

difference between the light and heavy atom is relatively minor and the ZPE approximation can break down. In those instances, EXC, MMI, and the TSDF may contribute substantially to the observed KIE. While the complexity of TSDF requires calculations of theoretical KIEs to determine the contribution of the TSDF,[70] EXC only significantly contributes to the KIE when the frequency (ν) of the bond of interest is less than 1500 cm^{-1}.[71] Previous work has shown that the NO bond in reduced hemoglobin and myoglobin has a frequency greater than 1500 cm^{-1},[92] while models of the Fe_B site revealed NO bond frequencies between 1720-1790 cm^{-1}.[91] Thus, it is likely that EXC is not a substantial contributor to the KIEs observed in cNOR.

MMI can be the prevailing contributor to the KIE under certain circumstances. Such a case occurs when the molecules of interest are small enough that isotopic substitution could substantially change the mass and moment of inertia.[70] While the small size of NO and modest magnitude of our observed KIE might suggest that MMI could be a major contributor to the KIEs, some KIE calculations have observed MMI does not significantly impact the overall KIE in reactions with early transition states (as proposed in the *cis*-heme b_3 mechanism).[93,94] Thus, calculation of all transition states and theoretical KIEs are needed to understand which component is dominant in our system.

CONCLUSIONS

In this manuscript we have presented the isotopic enrichment factors and KIEs of purified cNOR from *P. denitrificans*. A small normal isotope effect was observed for the ^{18}O, ^{15}N, and $^{15}N^{\beta}$, while no significant isotope effect was observed for the $^{15}N^{\alpha}$. By comparing our enzymatic S_P with the S_P from pure culture studies, we have provided further evidence that bacteria, like fungi,

hold NO at approximately steady-state levels resulting in a consistent S_P over time. While it is tempting to apply the ZPE approximation to our data to infer an enzymatic mechanism, the relatively small KIE values require a thorough computational analysis before more definitive mechanistic conclusions can be made.

ACKNOWLEDGMENT

We thank Nicolai Lenhert (University of Michigan) and Jennifer Dubois (Montana State University) for their helpful discussions.

APPENDIX

APPENDIX

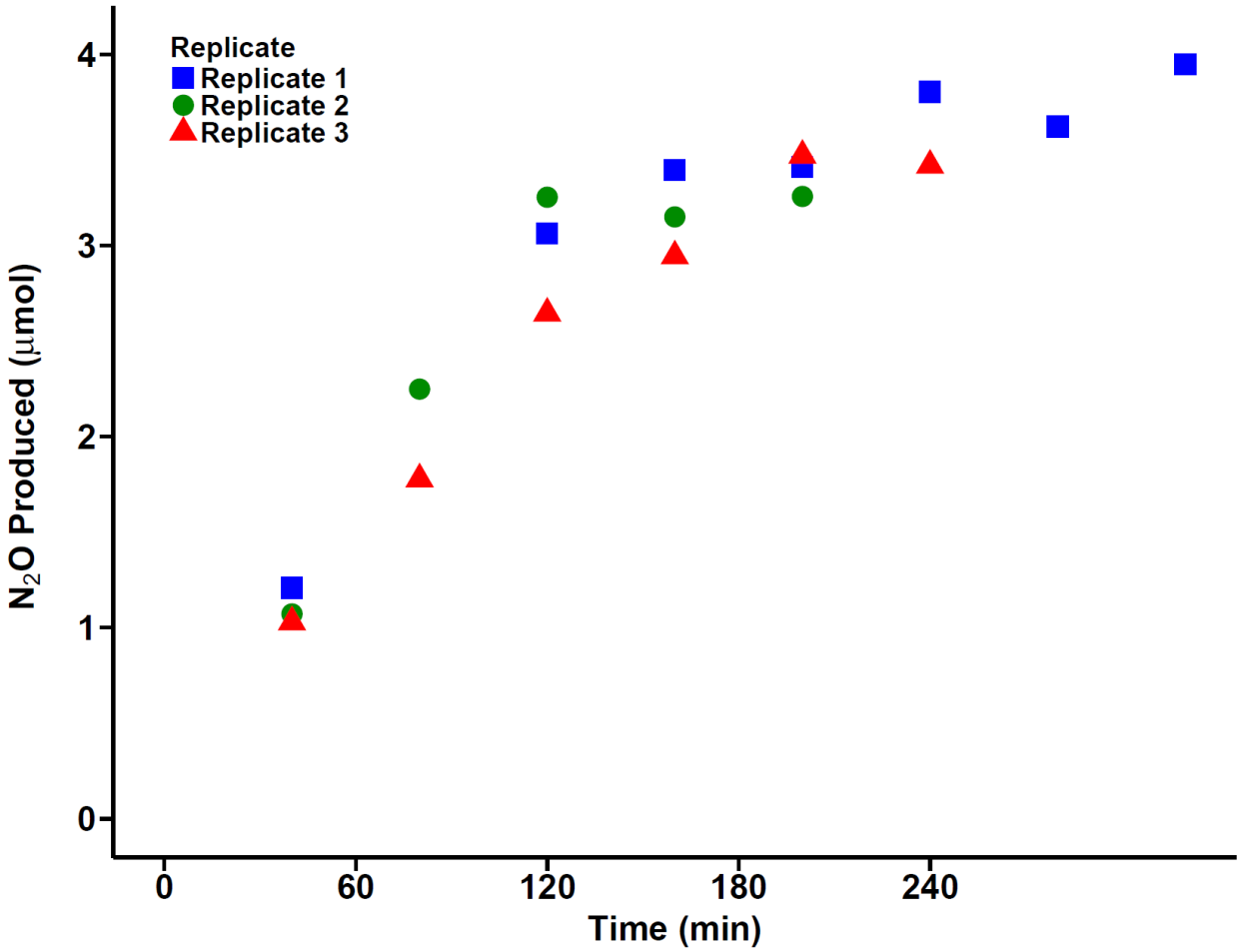

Figure 14. Production of N_2O by *P. denitrificans* cNOR with data points past 240 min included. All data points before individual replicates plateaued (Rep.1 before 280 min., Rep 2 before 160 min. and Rep 3. before 240 min.) were used in data analysis.

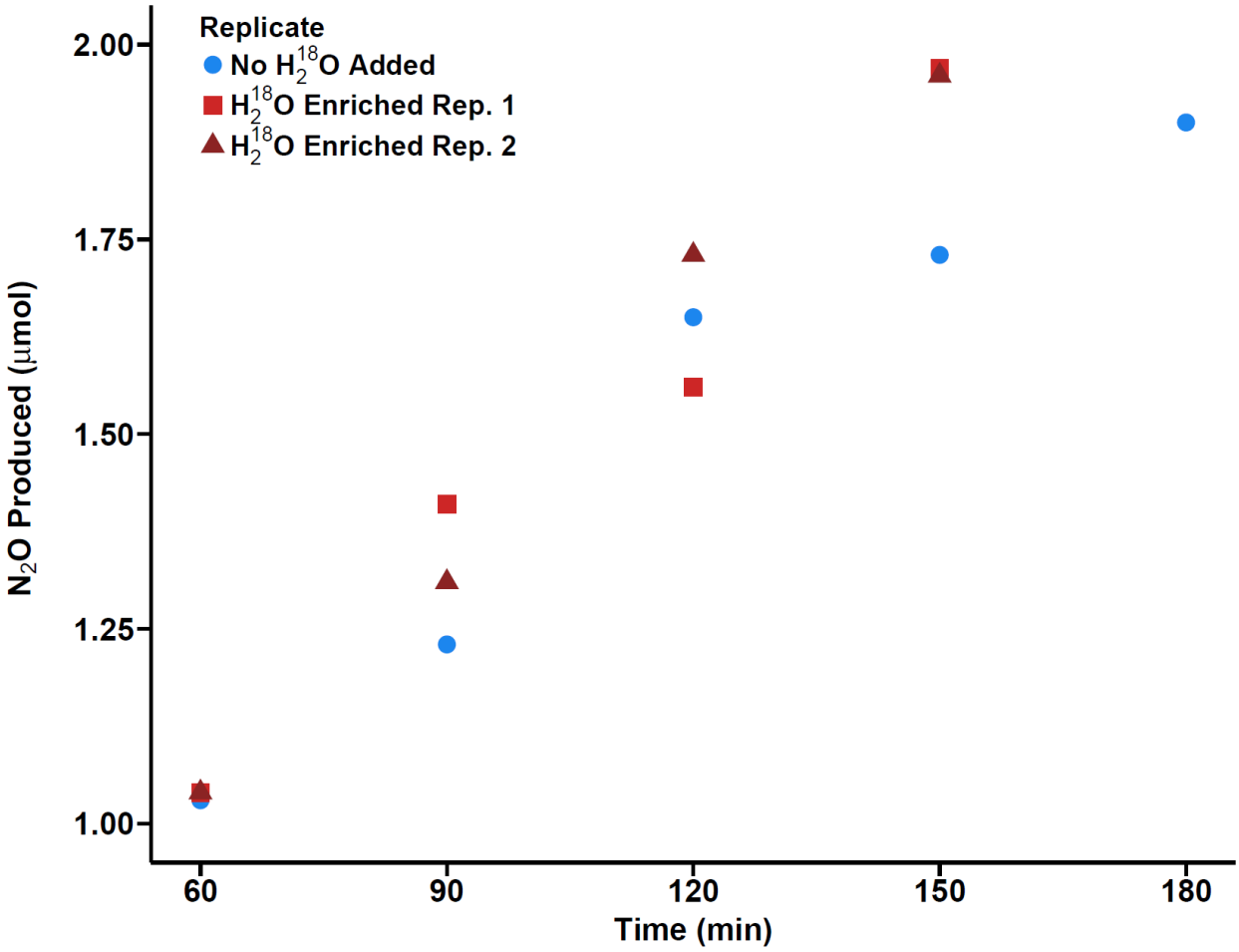

Figure 15. Production of N_2O by *P. denitrificans* cNOR with ^{18}O enriched water. Two replicates (red squares and dark red triangles) contained ^{18}O enriched water (87 ‰) while the third replicate (blue circles) did not. Each replicate contained 10.3 µmols of NO (g) and 78 nM cNOR. The maximum potential N_2O that could be produced was 5.15 µmols.

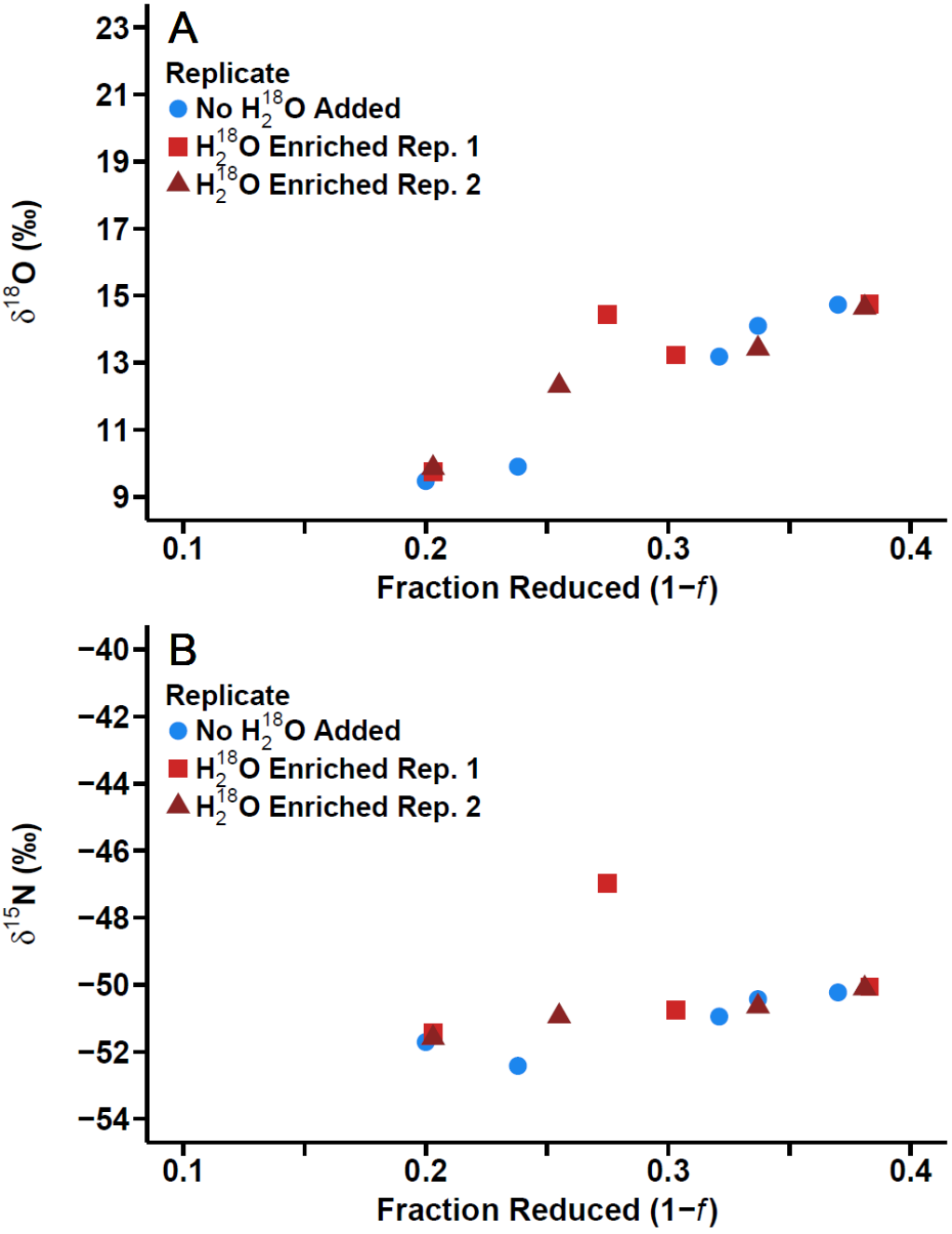

Figure 16 $\delta^{18}O$ (A) and $\delta^{15}N$ (B) of N_2O produced by three biological replicates as a function of the fraction of substrate (NO) reduced (1-f) with ^{18}O enriched water (red squares and dark red triangles) and unenriched water (blue circles).

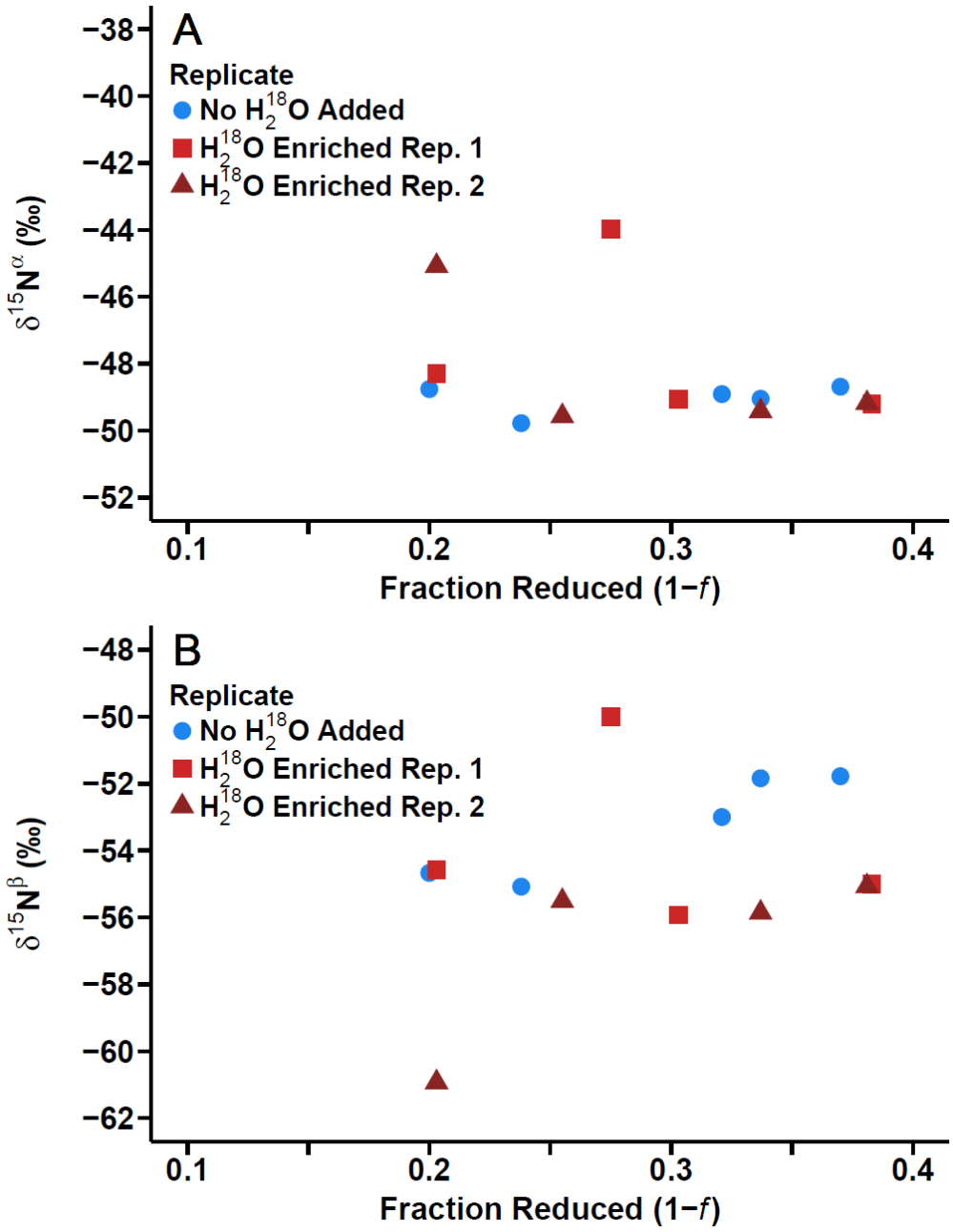

Figure 17. $\delta^{15}N^{\alpha}$ (A) and $\delta^{15}N^{\beta}$ (B) of N_2O produced by three biological replicates as a function of the fraction of substrate (NO) reduced (1-f) with ^{18}O enriched water (red squares and dark red triangles) and unenriched water (blue circles).

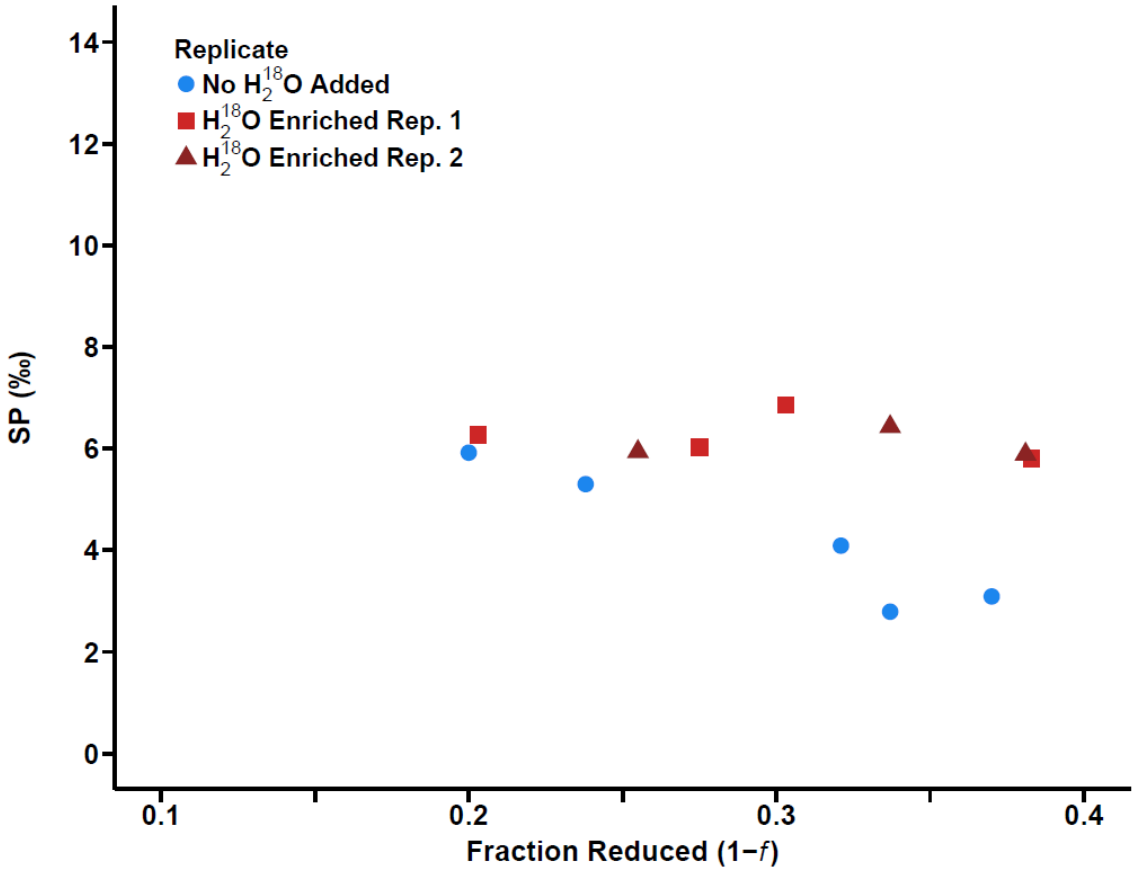

Figure 18. S_P ($S_P = \delta^{15}N^{\alpha} - \delta^{15}N^{\beta}$) for cNOR over the course of the enzymatic reaction) with ^{18}O enriched water (red squares and dark red triangles) and non-enriched water (blue circles). S_P is plotted against the fraction of substrate (NO) reduced with the reaction progressing from left to right. Three biological replicates were assayed.

Table 2. Enrichment factors (ε), p-values, R^2, and kinetic isotope effects of (KIEs) of *P. denitrificans* cNOR performed to test for ^{18}O exchange.

Measurement	Replicate	ε[a]	p-value	R^2
^{15}N	No $H_2{}^{18}O$ Added	-18.3	0.0447	0.7163
	$H_2{}^{18}O$ Enriched Rep. 1	-5.4	0.8716	0.4753
	$H_2{}^{18}O$ Enriched Rep. 2	-11.9	0.0291	0.914
$^{15}N^{\alpha}$	No $H_2{}^{18}O$ Added	-3.6	0.5431	-0.1535
	$H_2{}^{18}O$ Enriched Rep. 1	16.1	0.6943	-0.3599
	$H_2{}^{18}O$ Enriched Rep. 2	30.1	0.3021	0.2306
$^{15}N^{\beta}$	No $H_2{}^{18}O$ Added	-32.9	0.0165	0.8503
	$H_2{}^{18}O$ Enriched Rep. 1	12.9	0.7716	-0.4218
	$H_2{}^{18}O$ Enriched Rep. 2	-42.4	0.2252	0.4005
^{18}O	No $H_2{}^{18}O$ Added	-54.3	0.0013	0.9715
	$H_2{}^{18}O$ Enriched Rep. 1	-40.3	0.1776	0.5144
	$H_2{}^{18}O$ Enriched Rep. 2	-39.2	0.034	0.8997
SP	No $H_2{}^{18}O$ Added	29.3	0.0109	0.8862
	$H_2{}^{18}O$ Enriched Rep. 1	3.2	0.6666	-0.3332
	$H_2{}^{18}O$ Enriched Rep. 2	72.5	0.2561	0.3301

[a] While ε, p-values, and R^2 coefficients are provided, due to the small *f* range in the data, the ε cannot be taken as an accurate measurement of the entire reaction.

.

CHAPTER 3: New Dog, Old Tricks: Isotopic Studies of a Cytochrome *c* Nitric Oxide Reductase (cNOR) Mimic

Clarisse M. Finders[†], Joshua A. Haslun[†], Hasand Gandhi[‡], Peggy H. Ostrom[‡], Nathaniel E. Ostrom[‡,], Eric L. Hegg[†,]**

Joshua Haslun and Hasand Gandhi helped with experiment design and isotope ratio analysis of the N_2O molecules. Peggy Ostrom helped with analyzing the data. Nathaniel Ostrom and Eric Hegg helped with data analysis and directed the research.

ABSTRACT

Unlike many other nitrogen species, nitrous oxide (N_2O) is a powerful greenhouse gas (100-year global warming potential ~265 times that of carbon dioxide) and is the major pathway of stratospheric ozone destruction. Because approximately half of all N_2O formed in a given year is the result of various human activities, it is necessary to identify and mitigate anthropogenic sources of N_2O. The single largest source of anthropogenic N_2O is due to fertilization practices, which exacerbates the microbial process of denitrification. In denitrification, NO_3^- and NO_2^- are reduced to N_2, with N_2O produced as an obligate intermediate. N_2O is directly produced by the enzyme nitric oxide reductase (NOR), which catalyzes the conversion of NO to N_2O. The most well-known bacterial NOR is the cytochrome *c* NOR (cNOR), which contains multiple metal centers and is an integral membrane protein, making it challenging to study. In an effort to gain

more insight into the mechanism of cNOR, the Yi Lu lab at the University of Illinois Urbana-Champaign mutated sperm whale myoglobin (Mb) to generate a mimic of cNOR. The mimic, called I107EFe_BMb, has been shown to be a structural and functional model of the NOR active site and is capable of producing N_2O. To further establish the accuracy of I107EFe_BMb as a model of cNOR, we attempted to determine the isotopic enrichment factor (ε) and kinetic isotope effects (KIEs) of I107EFe_BMb to compare them to the values we previously obtained for cNOR. While I107EFe_BMb did produce N_2O, the limited extent of reaction we observed prevented us from calculating ε values or the KIEs of I107EFe_BMb. The isotopic data that was gathered are presented along with a discussion of future possibilities to extend the *f* range and obtain ε values and KIEs.

INTRODUCTION

Nitrous oxide (N_2O) is an obligate intermediate in denitrification, a process in which NO_3^- and NO_2^- are reduced to N_2. N_2O is also a potent greenhouse gas, having a 100-year global warming potential ~265 times greater than that of carbon dioxide.[1] Approximately half of all N_2O emitted per year is anthropogenically produced and, of the anthropogenic N_2O, ~80% is the result of agricultural practices.[95,38] Excess fertilization stimulates a range of microbial nitrogen cycling processes that can produce N_2O. One of these is bacterial denitrification which has been cited as the predominant source of N_2O emissions in agricultural soils.[29] Mitigation strategies therefore should not only examine the microbes that produce N_2O, but also the enzymes that directly catalyze N_2O formation.

The enzyme responsible for reducing NO to N_2O in bacterial denitrification is termed nitric oxide reductase. Currently the most well studied bacterial NOR is cNOR, which is named for its natural reductant cytochrome *c.* cNOR is an integral membrane protein that consists of two subunits, NorC and NorB. NorC contains a single heme *c* that serves to pass electrons between cytochrome *c* and NorB, where catalysis occurs. NorB is comprised of 12 transmembrane helices, a calcium ion, two heme *b* molecules, and a non-heme Fe, termed Fe_B. Once the heme *c* in NorC receives an electron, the electron is passed to one of the *b*-type hemes in NorB. The first heme *b* then passes electrons to the second heme *b* in NorB. This second heme *b,* called heme b_3, serves as half of the catalytic site, with Fe_B as the other half.[75] While there has been great interest in the cNOR mechanism for many years, a single mechanism has not yet been agreed upon.[52,51] This is due in part to the difficulties of isolating and purifying membrane proteins and the spectroscopic challenges associated with multiple metal centers in one protein.

Recognizing the need for a simplified cNOR mimic that could be produced in large quantities, Yeung *et al.* engineered a cNOR mimic from sperm whale myoglobin (Mb) in 2009.[89] The mimic, called Fe_BMb, was produced by engineering an iron binding site into Mb by mutating three residues to histidines and a glutamate (L29H, F43H, V68E). Ultra violet-visible (UV-Vis) spectroscopy confirmed iron binding to the engineered site and EPR spectroscopy revealed spin-coupling between the heme iron and non-heme iron, as is observed in cNOR. More impressively, Fe_BMb was able to reduce NO to N_2O, demonstrating that it is both an active site structural model and a functional mimic of cNOR.[89]

Further improvement of the model was made when a second glutamate was introduced into Fe_BMb, resulting in a new enzyme termed I107EFe_BMb. This mimic increased total NO → N_2O conversion from ~10% to ~24% N_2O production, revealing the importance of the second

conserved glutamate in cNOR. It is hypothesized that this second Glu enhances proton uptake in I107EFe_BMb, as it was seen that I107E interacts with a water molecule in the crystal structure. Rapid-freeze-quench Raman spectroscopy studies further highlighted the importance of the second glutamate as it was found that this glutamate prevents the formation of a dead-end complex seen in the Fe_BMb enzymes.[96] By replacing Fe with Cu or Zn in the Fe_B site, it was shown that the metal in the Fe_B site influences the reduction potential of the heme.[59] In the Fe_BMb enzymes, exposure to excess NO leads to a five coordinate heme-nitrosyl complex that does not yield N_2O formation. It was determined that this dead-end complex was the result of a second NO molecule displacing the proximal histidine to the heme. It was suggested that this five coordinate intermediate is avoided in I107EFe_BMb due to the second glutamate protonating the NO bound on the distal side of the heme.[96]

To further elucidate the mechanism by which I107EFe_BMb produces NO, any chemistry occurring at Fe_B site can be examined by replacing the native heme in Mb with other protoporphyrins. Chakraborty *et al.* replaced the native heme with Zn protoporphyrin IX (ZnPP) and examined the chemistry occurring at the Fe_B site. Mössbauer and EPR spectroscopy of ZnPPFe_BMb1 with NO showed the formation of a radical bound to the Fe in the Fe_B site. These data, taken together with the previous studies that reveal NO binding to the heme in I107EFe_BMb, lend support to the *trans* mechanism proposed to cNOR.[97]

Given the evidence that I107EFe_BMb is a good mimic of cNOR, we performed experiments with the goal of determining the isotopic enrichment factors (ε) and KIEs of I107EFe_BMb to gain mechanistic insights into the reaction catalyzed by this mimic. A second goal was to examine the mechanistic similarity of I107EFe_BMb and the native cNOR by comparing the KIEs obtained from these two enzymes. Because the enzyme is only capable of a single turnover, however, the

extent of reaction was not sufficient to accurately determine either ε values or the KIEs. The N_2O production and isotopic data that were collected is presented and discussed in the following sections.

MATERIALS AND METHODS

NO Solution Preparation

An NO solution was prepared by attaching a 160 mL side arm flask containing degassed water and two stainless steel traps (20 cm x 0.6 cm) to a cylinder of 99.5% NO (Airgas). The molecular sieve (5A, 8 x 12 mesh; Arcos Organics) and Ascarite II (20-30 mesh, Thomas Scientific) contained in the traps were heated overnight under vacuum to degas and precondition that trap material (180 °C and ~10^{-2} Torr, respectively). After cooling the traps to room temperature, NO was allowed to flow through the traps and enter the degassed water in the side arm flask. The concentration of the NO solution was determined according to the assay by Hogg and Kalyanaraman.[98] The concentration of the NO solution was found to be 0.33 mM. All glassware was washed in both acid and base baths prior to experiments. I107EFe_BMb was generously provided by Professor Lu (University of Illinois, Urbana-Champaign).

Enzymatic Assays: I107EFe_BMb (25 nmol) was reduced with 1.77equivalents of sodium dithionite in an anaerobic chamber (Coy). Excess dithionite was removed using a desalting column (PD MiniTrap^{TM} G-25, GE Healthcare) that had been equilibrated with 100 mL of degassed 50 mM Bis-Tris propane buffer (pH 7.1, Sigma-Aldrich, 10 mL of 0.25 mM dithionite spiked buffer and 90 mL unspiked buffer). Two equivalents of $FeSO_4 \cdot 7\ H_2O$ (Mallinckrodt) were added to the collected enzyme fraction, and the solution was transferred to a 13 mL serum vial.

After the serum vial was capped with a butyl stopper (Geo-Microbial Technologies, Inc.) and crimped, the reaction was initiated by injecting 240 μL of NO solution (80 nmol) into the serum vial using a gastight syringe (Hamilton).

Controls were performed in duplicate to determine if abiotic N_2O production was occurring. Because one equivalent of both dithionite and Fe^{2+} is required for enzyme activity, the controls contained only the excess of these reagents. 0.77 equivalents of sodium dithionite was run through a column and collected. One equivalent of $FeSO_4 \cdot 7\ H_2O$ was added to the collected fraction and the solution was transferred to a 13 mL serum vial. The vial was capped, crimped, and NO solution was added (80 nmol, 240 μL of solution) to initiate the reaction. Both the controls and enzymatic reactions were constantly shaken at 100 rpm at 30°C during the course of the reactions.

To determine the amount and isotopic composition of the N_2O produced, the samples and controls were analyzed on an isotope ratio mass spectrometer (IRMS) as previously described in Chapter 2. The definition of δ values and the Toyoda and Yoshida corrections were applied in the same way presented in Chapter 2, and the delta (δ) values for our laboratory pure N_2O standards for $\delta^{18}O$, $\delta^{15}N$, $\delta^{15}N^{\alpha}$, and $\delta^{15}N^{\beta}$ are the same as in the previous chapter. In the Rayleigh model, the two variables that are plotted against each other are the δ value obtained for the product (y-axis) and $-f*\ln f/(1-f)$, (x axis) with f being the fraction of substrate remaining The range in f is synonymous with the extent of the reaction. Therefore, ε (the slope of the line) and the KIE (derived from ε), will be most accurate when the largest extent of reaction is captured. Because the enzyme mimic is presently capable of only a single turnover, we simulated an f range by making individual reactions at different time points (18, 26, 33, 43, and 53 hours), with

each time point assayed in triplicate. Because it was only possible to perform two assays due to limited enzyme, statistical tests were not performed on the obtained data.

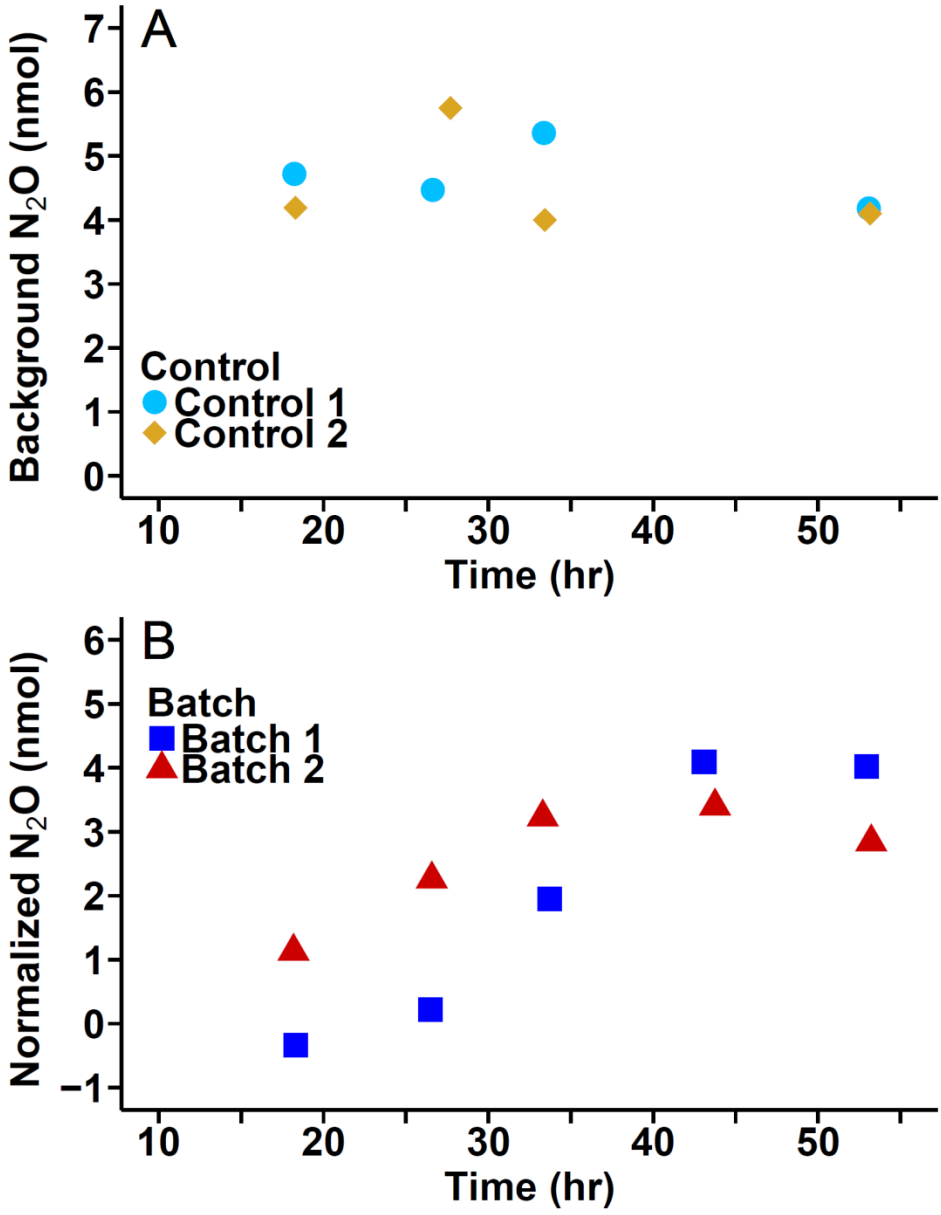

Figure 19. Production of N_2O from NO controls and I107EFe$_B$Mb reactions. (A) N_2O observed in controls at 18, 26, 33, and 53 hours. No controls were made for the 43-hour time point. (B) N_2O produced by I107EFe$_B$Mb experiments after subtracting out the average background N_2O from the controls.

Enzymatic N_2O Production

The production of N_2O by both the controls and I107EFe_BMb was obtained from the samples and analyzed on the IRMS. As can be seen in Figure 19 (A), the amount of N_2O in the controls remained fairly constant over time. Because there is no clear increase in N_2O production, we believe that this N_2O is most likely simply background in the NO stock solution and not the result of abiotic reactions.

To be consistent in our analysis, the average amount of N_2O in all of the controls was subtracted from the N_2O observed in the I107EFe_BMb assays, yielding a normalized N_2O amount (Figure 19 (B)). A marked increase in N_2O can be seen in both samples up to ~43 hours at which point N_2O production plateaus. There appears to be a difference in production rates between the two batches of I107EFe_BMb analyzed. While Batch 1 began producing N_2O later than Batch 2, Batch 1 produced slightly more product. One explanation for this is that these are different sample preparations and therefore not exactly the same. Overall, I107EFe_BMb is capable of catalyzing NO reduction, albeit at an extremely slow rate compared to the native enzyme.

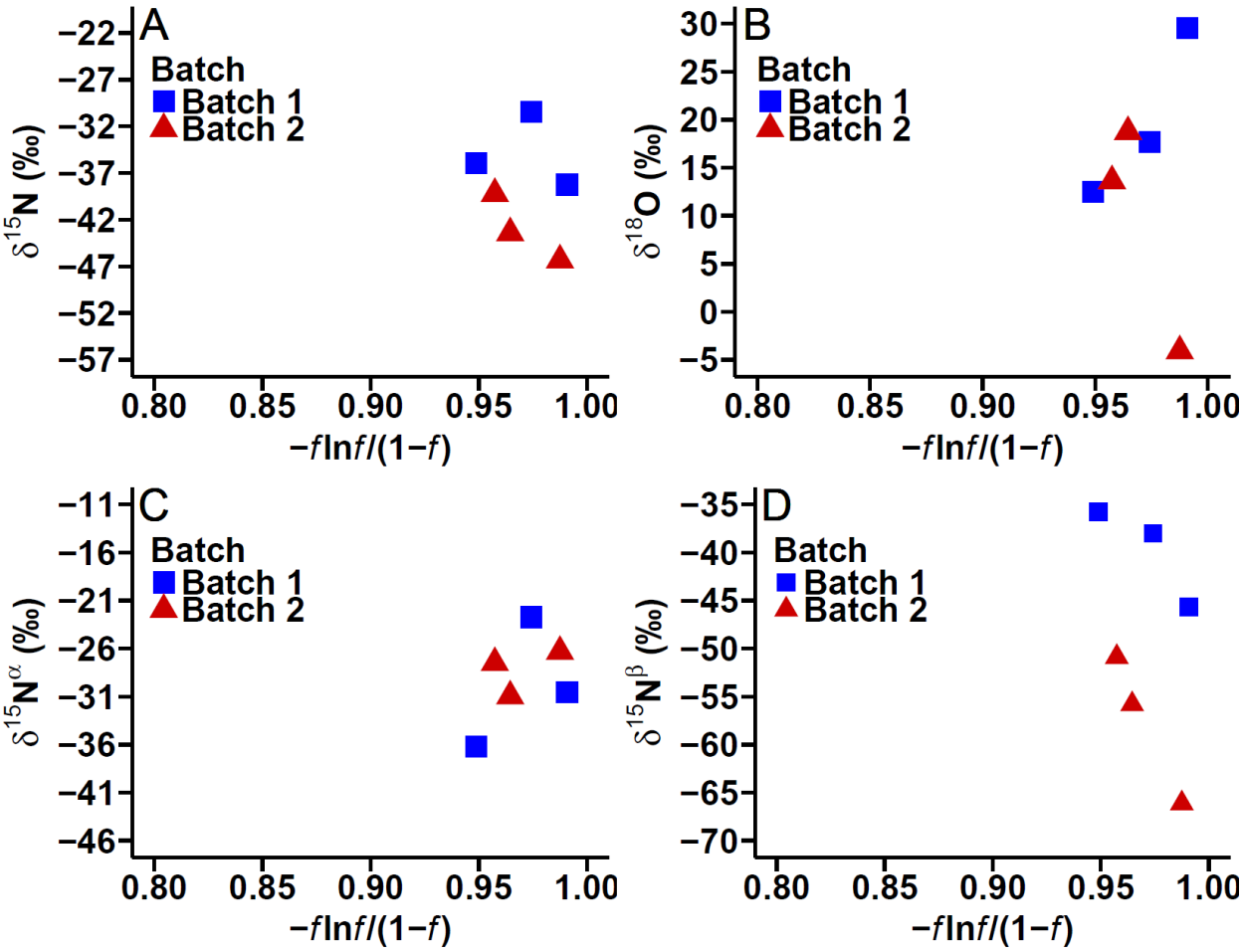

Figure 20. Isotopic fractionation of bulk nitrogen (A), oxygen (B), N^{α} (middle nitrogen, C), and N^{β} (terminal nitrogen, D). All isotope ratios are plotted against the fraction of substrate (NO) remaining progressing from right to left. Two batches of I107EFe_BMb were assayed.

Assessment of $\delta^{15}N$, $\delta^{18}O$, $\delta^{15}N^{\alpha}$, and $\delta^{15}N^{\beta}$ of N_2O produced by I107EFe_BMb

Isotope values ($\delta^{15}N$, $\delta^{18}O$, $\delta^{15}N^{\alpha}$, and $\delta^{15}N^{\beta}$) were measured for the reduction of NO to N_2O by I107EFe_BMb during 5 different time points. All results only span a range of ~5% conversion of substrate to product, greatly limiting the conclusions that can be drawn and making it impractical to determine S_P, ε, and KIEs. It is interesting to note that there appears to be the beginning of a

trend in the data. For example, if the data for the bulk nitrogen (Figure 20A) are taken all together, a positive trend may be present. In the oxygen data on the other hand (Figure 20B), a downward trend (ignoring one point) seems to be present. There does not seem to be a trend emerging in the N^{α} (Figure 20C), while the N^{β} (Figure 20D) may have a general negative trend, similar to the bulk nitrogen. It must be reemphasized, however, that the very small *f* range does not allow any concrete conclusions to be drawn. The unrealistically large δ ranges also reinforce the dangers of drawing conclusions from an *f* range this small.

There are a few ways a larger *f* range could be accomplished. One strategy is to purge any background N_2O so as to be certain that all N_2O observed in the I107EFe_BMb reactions was produced by the protein. While it might be tempting to raise the NO concentration to increase the probability of NO binding to I107EFe_BMb, *f* is defined as the fraction of substrate remaining. Therefore increasing the NO would only yield an even smaller *f* range. One of the greatest barriers to a large *f* range is the single turnover limitation of I107EFe_BMb. It may be possible to achieve multiple turnovers by supplying excess reductant. Because dithionite produces N_2O abiotically (data not shown), however, it is not possible to add excess dithionite to the reactions. Cysteine, NADH, ascorbate, glyceraldehyde, and hydroquinone have all been used as reductants for metmyoglobin in the past.[99] If one of these molecules could reduce I107EFe_BMb and does not produce N_2O on its own, then it may be possible to achieve multiple turnovers for I107EFe_BMb without simply increasing the abiotic reduction of NO. Further work needs to be done to examine this possibility.

In this chapter, we have examined the N_2O production and isotopic fractionation of a cNOR mimic, I107EFe_BMb. While I107EFe_B is capable of reducing NO to N_2O, the limited extent of the reaction we observed does not allow us to make any definitive conclusions about either the

isotopic fractionation or the mechanism of I107EFe_BMb. Future studies examining different reductants and improving the turnover number of the enzyme will need to be accomplished before accurate isotopic information can be gathered.

ACKNOWLEDGMENT

We thank Julian Reed (University of Illinois Urbana-Champaign) for his help with the I107EFe_BMb assays and providing protein.

CHAPTER 4:Knowledge Gained and Next Steps

In this thesis I have presented two studies examining N_2O biosynthesis and isotopic fractionation from two different systems: a natural cytochrome *c* nitric oxide reductase or cNOR (Chapter 2) and an engineered cNOR mimic, I107EFe_BMb (Chapter 3) using isotope ratio mass spectrometry.

Our results revealed that the native cNOR from *Paracoccus denitrificans* discriminates against the heavy isotope for the oxygen, N^{β}, and the bulk nitrogen while no discrimination between the two isotopes is observed for the N^{α}. Three important conclusions were made from these results. The first is that while our data are consistent with either of the two proposed *cis* mechanisms, we are not able to definitively rule out the proposed *trans* mechanism due to the small magnitude of our isotope effects. The magnitude of our observed KIEs leads to the second conclusion, which is that the zero-point energy difference between the two isotopes may not be the dominant contributor to the final KIE. Other factors, such as the mass moment of inertia (MMI) or transition state decomposition frequency (TSDF) may be contributing significantly to the observed KIE. KIE calculations of the transition states for all of the proposed mechanisms will be necessary to pinpoint the predominant contributor. Other future experiments include examining the isotopic composition of N_2O produced from purified quinol NOR (qNOR). As qNOR and cNOR have a high degree of sequence similarity and presumably follow an identical reaction mechanism[62], the isotopic fractionations would be expected to be similar. If the KIEs from qNOR displayed similar trends as cNOR but were larger in magnitude, more refined mechanistic conclusions could be made. Finally, in our study of cNOR we demonstrated that under our reaction conditions, oxygen exchange between water and NO does not occur. This

implies that any oxygen exchange that does occur during denitrification takes place before the formation of N_2O.

In our experiments with I107EFe_BMb, measurable N_2O production was detected. However, the extremely short extent of reaction that was captured did not allow for accurate determination of isotopic enrichment factors and KIEs. The isotopic data that were obtained could indicate the beginnings of trends, but without further experiments it is impossible to say for certain. Future experiments with I107EFe_BMb will focus on improving N_2O production. This could be accomplished through tuning the binding of I107EFe_BMb to the substrate/Fe_B so that more of the enzyme mimic turned over under single turnover conditions. N_2O production could also be improved by changing the assay conditions to promote multiple turnovers so that this sample becomes a true enzyme.

REFERENCES

REFERENCES

(1) Myher, G., Shindell, D., Breon, F. M., Collins, W., Fuglestvedt, J., Huang, D., Koch, J., Lamarque, F., Lee, D., Mendoza, B., Nakajima, T., Robock, A., Stephens, G., Takemura, T., and Zhang, H. (2013) Anthropogenic and Natural Radiative Forcing, in *Climate Change 2013: The Phycsical Science Basis. Contribution of Working Group I to the Fifth Assescment Report of the Intergovernmental Panel on Climate Change* (Stocker, T. F., Qin, D., Plattner, G. K., Tignor, M., Allen, S. K., Boschung, J., Nauels, A., Bex, V., and Midgley, P. M., Eds.), pp 73–79. Cambridge University Press, Cambridge, UK.

(2) Galloway, J. N., Aber, J. D., Erisman, J. W., Seitzinger, S. P., Howarth, R. W., Cowling, E. B., and Cosby, B. J. (2003) The Nitrogen Cascade. *Bioscience 53*, 341–356.

(3) Denk, T. R. A., Mohn, J., Decock, C., Lewicka-Szczebak, D., Harris, E., Butterbach-Bahl, K., Kiese, R., and Wolf, B. (2017) The nitrogen cycle: A review of isotope effects and isotope modeling approaches. *Soil Biol. Biochem. 105*, 121–137.

(4) Fowler, D., Coyle, M., Skiba, U., Sutton, M. A., Cape, J. N., Reis, S., Sheppard, L. J., Jenkins, A., Grizzetti, B., Galloway, N., Vitousek, P., Leach, A., Bouwman, A. F., Butterbach-bahl, K., Dentener, F., Stevenson, D., Amann, M., Voss, M., and Fowler, D. (2013) The global nitrogen cycle in the twenty- first century. *Philisophical Trans. R. Soc. B.*

(5) Bond, A. L., and Hobson, K. A. (2012) Reporting Stable-Isotope Ratios in Ecology: Recommended Terminology, Guidelines and Best Practices. *Waterbirds 35*, 324–331.

(6) Ostrom, N. E., and Ostrom, P. H. (2012) The Isotopomers of Nitrous Oxide: Analytical Considerations and Application to Resolution of Microbial Production Pathways, in *Handbook of Environmental Isotope Geochemistry*, pp 453–476.

(7) Mariotti, A., Germon, J. C., Hubert, P., Kaiser, P., Letolle, R., Tardieux, A., and Tardieux, P. (1981) Experimental determination of nitrogen kinetic isotope fractionation: Some principles; illustration for the denitrification and nitrification processes. *Plant Soil 62*, 413–430.

(8) Hoffman, B. M., Lukoyanov, D., Yang, Z. Y., Dean, D. R., and Seefeldt, L. C. (2014) Mechanism of nitrogen fixation by nitrogenase: The next stage. *Chem. Rev. 114*, 4041–4062.

(9) Eady, R. R. (1996) Structure-function relationships of alternative nitrogenases. *Chem. Rev. 96*, 3013–3030.

(10) Hu, Y., and Ribbe, M. W. (2011) Biosynthesis of nitrogenase FeMoco. *Coord. Chem. Rev. 255*, 1218–1224.

(11) Nørskov, J., Chen, J., Miranda, R., Fitzsimmons, T., and Stack, R. (2016) Sustainable Ammonia Synthesis – Exploring the scientific challenges associated with discovering alternative, sustainable processes for ammonia production.

(12) Macko, S. A., Fogel, M. L., Hare, P. E., and Hoering, T. C. (1987) Isotopic fractionation of nitrogen and carbon in the synthesis of amino acids by microorganisms. *Chem. Geol. Isot. Geosci. Sect. 65*, 79–92.

(13) Bauersachs, T., Schouten, S., Compaore, J., Wollenzien, U., Stal, L. J., and Sinninghe Damste, J. S. (2009) Nitrogen isotopic fractionation associated with growth on dinitrogen gas and nitrate by cyanobacteria. *Limnol. Oceanogr. 54*, 1403–1411.

(14) Zhang, X., Sigman, D. M., Morel, F. M. M., and Kraepiel, A. M. L. (2014) Nitrogen isotope fractionation by alternative nitrogenases and past ocean anoxia. *Proc. Natl. Acad. Sci. 111*, 4782–4787.

(15) Focht, D. D., and Verstraete, W. (1977) Biochemical Ecology of Nitrification and Denitrification, in *Advances in Microbial Ecology* (Alexander, M., Rosswall, T., Shilo, M., and Veldkamp, H., Eds.), pp 135–214. Plenum Press, New York.

(16) Cai, M., Ng, S.-K., Lim, C. K., Lu, H., Jia, Y., and Lee, P. K. H. (2018) Physiological and Metagenomic Characterizations of the Synergistic Relationships between Ammonia- and Nitrite-Oxidizing Bacteria in Freshwater Nitrification. *Front. Microbiol. 9*, 1–13.

(17) Caranto, J. D., and Lancaster, K. M. (2017) Nitric oxide is an obligate bacterial nitrification intermediate produced by hydroxylamine oxidoreductase. *Proc. Natl. Acad. Sci. 114*, 8317–8222.

(18) Kuypers, M. M. M., Marchant, H. K., and Kartal, B. (2018) The microbial nitrogen-cycling network. *Nat. Rev. Microbiol.*

(19) Hu, H. W., and He, J. Z. (2017) Comammox—a newly discovered nitrification process in the terrestrial nitrogen cycle. *J. Soils Sediments 17*, 2709–2717.

(20) Jetten, M. S. M., Wagner, M., Fuerst, J., Van Loosdrecht, M., Kuenen, G., and Strous, M. (2001) Microbiology and application of the anaerobic ammonium oxidation ('anammox') process. *Curr. Opin. Biotechnol. 12*, 283–288.

(21) Jin, R. C., Yang, G. F., Yu, J. J., and Zheng, P. (2012) The inhibition of the Anammox process: A review. *Chem. Eng. J. 197*, 67–79.

(22) Brunner, B., Contreras, S., Lehmann, M. F., Matantseva, O., Rollog, M., Kalvelage, T., Klockgether, G., Lavik, G., Jetten, M. S. M., Kartal, B., and Kuypers, M. M. M. (2013) Nitrogen isotope effects induced by anammox bacteria. *Proc. Natl. Acad. Sci. 110*, 18994–18999.

(23) Burgin, A. J., and Hamilton, S. K. (2007) Have we overemphasized the role of denitrification in aquatic ecosystems ? A review of nitrate removal pathways. *Front. Ecol. Environ. 5*, 89–96.

(24) Tiedje, J. M., Sexstone, A. J., Myrold, D. D., and Robinson, J. A. (1983) Denitrification: ecological niches, competition and survival. *Antonie Van Leeuwenhoek 48*, 569–583.

(25) Rütting, T., Boeckx, P., Müller, C., and Klemedtsson, L. (2011) Assessment of the importance of dissimilatory nitrate reduction to ammonium for the terrestrial nitrogen cycle. *Biogeosciences 8*, 1779–1791.

(26) Silver, W. L., Herman, D. J., Firestone, M. K., and Sep, N. (2012) Dissimilatory Nitrate Reduction to Ammonium in Upland Tropical Forest Soils. *Ecology 82*, 2410–2416.

(27) Wrage, N., Velthof, G. L., Van Beusichem, M. L., and Oenema, O. (2001) Role of nitrifier denitrification in the production of nitrous oxide. *Soil Biol. Biochem. 33*, 1723–1732.

(28) Tavares, P., Pereira, A. S., Moura, J. J. G., and Moura, I. (2006) Metalloenzymes of the denitrification pathway. *J. Inorg. Biochem. 100*, 2087–2100.

(29) Zumft, W. G. (1997) Cell Biology and Molecular Basis of Denitrification. *Microbiol. Mol. Biol. Rev. 61*, 533–616.

(30) Baggs, E. M. (2011) Soil microbial sources of nitrous oxide: Recent advances in knowledge, emerging challenges and future direction. *Curr. Opin. Environ. Sustain. 3*, 321–327.

(31) Shoun, H., Fushinobu, S., Jiang, L., Kim, S.-W., and Wakagi, T. (2012) Fungal denitrification and nitric oxide reductase cytochrome P450nor. *Philos. Trans. R. Soc. B Biol. Sci. 367*, 1186–1194.

(32) Spott, O., Russow, R., and Stange, C. F. (2011) Formation of hybrid N_2O and hybrid N_2 due to codenitrification: First review of a barely considered process of microbially mediated N-nitrosation. *Soil Biol. Biochem. 43*, 1995–2011.

(33) Yang, H., Gandhi, H., Ostrom, N. E., and Hegg, E. L. (2014) Isotopic Fractionation by a Fungal P450 Nitric Oxide Reductase during the Production of N_2O. *Environ. Sci. Technol. 48*, 10707–10715.

(34) Van Breemen, N., Boyer, E. W., Goodale, C. L., Jaworski, N. A., Paustian, K., Seitzinger, S. P., Lajtha, K., Mayer, B., Van Dam, D., Howarth, R. W., Nadelhoffer, K. J., Eve, M., and Billen, G. (2002) Where did all the nitrogen go? Fate of nitrogen inputs to large watersheds in the northeastern U.S.A. *Biogeochemistry 57–58*, 267–293.

(35) Sutka, R. L., Ostrom, N. E., Ostrom, P. H., Breznak, J. A., Gandhi, H., Pitt, A. J., and Li, F. (2006) Distinguishing Nitrous Oxide Production from Nitrification and Denitrification on the Basis of Isotopomer Abundances. *Appl. Environ. Microbiol. 72*, 638–644.

(36) Sutka, R. L., Adams, G. C., Ostrom, N. E., and Ostrom, P. H. (2008) Isotopologue fractionation during N_2O production by fungal denitrification. *Rapid Commun. Mass Spectrom. 22*, 3989–3996.

(37) Haslun, J. A., Ostrom, N. E., Hegg, E. L., and Ostrom, P. H. (2017) Estimation of isotopologue variation of N_2O during denitrification by *Pseudomonas aureofaciens* and *Pseudomonas chlororaphis*: Implications for N_2O source apportionment. *Biogeosciences Discuss.* in review.

(38) Evironmental Protection Agency. (2015) Nitrous Oxide Emissions. *https://www.epa.gov/ghgemissions/overview-greenhouse-gases*

(39) Frey, S. D., Elliott, E. T., and Paustian, K. (1999) Bacterial and fungal abundance and biomass in conventional and no-tillage agroecosystems along two climatic gradients. *Soil Biol. Biochem. 31*, 573–585.

(40) Hendriks, J., Oubrie, A., Castresana, J., Urbani, A., Gemeinhardt, S., and Saraste, M. (2000) Nitric oxide reductases in bacteria. *Biochim. Biophys. Acta - Bioenerg. 1459*, 266–273.

(41) Gomes, C. M., Giuffrè, A., Forte, E., Vicente, J. B., Saraiva, L. M., Brunori, M., and Teixeira, M. (2002) A novel type of nitric-oxide reductase: *Escherichia coli* flavorubredoxin. *J. Biol. Chem. 277*, 25273–25276.

(42) Wang, J., Vine, C. E., Balasiny, B. K., Rizk, J., Bradley, C. L., Tinajero-Trejo, M., Poole, R. K., Bergaust, L. L., Bakken, L. R., and Cole, J. A. (2016) The roles of the hybrid cluster protein, Hcp and its reductase, Hcr, in high affinity nitric oxide reduction that protects anaerobic cultures of *Escherichia coli* against nitrosative stress. *Mol. Microbiol. 100*, 877–892.

(43) Romão, C. V., Vicente, J. B., Borges, P. T., Victor, B. L., Lamosa, P., Silva, E., Pereira, L., Bandeiras, T. M., Soares, C. M., Carrondo, M. A., Turner, D., Teixeira, M., and Frazão, C. (2016) Structure of *Escherichia coli* Flavodiiron Nitric Oxide Reductase. *J. Mol. Biol. 428*, 4686–4707.

(44) Khatua, S., and Majumdar, A. (2015) Flavodiiron nitric oxide reductases: Recent developments in the mechanistic study and model chemistry for the catalytic reduction of NO. *J. Inorg. Biochem. 142*, 145–153.

(45) Heiss, B., and Frunzke Zumft, K. W. G. (1989) Formation of the N-N bond from nitric oxide by a membrane-bound cytochrome *bc* complex of nitrate-respiring (denitrifying) *Pseudomonas stutzeri*. *J. Bacteriol. 171*, 3288–3297.

(46) Field, S. J., Thorndycroft, F. H., Matorin, A. D., Richardson, D. J., and Watmough, N. J. (2008) The Respiratory Nitric Oxide Reductase (NorBC) from *Paracoccus denitrificans*. *Methods Enzymol.* Elsevier Masson SAS.

(47) van der Oost, J., de Boer, a P., de Gier, J. W., Zumft, W. G., Stouthamer, a H., and van Spanning, R. J. (1994) The heme-copper oxidase family consists of three distinct types of terminal oxidases and is related to nitric oxide reductase. *FEMS Microbiol. Lett. 121*, 1–9.

(48) Shiro, Y., Sugimoto, H., Tosha, T., Nagano, S., and Hino, T. (2012) Structural basis for nitrous oxide generation by bacterial nitric oxide reductases. *Philos. Trans. R. Soc. B-Biological Sci. 367*, 1195–1203.

(49) Hino, T., Matsumoto, Y., Nagano, S., Sugimoto, H., Fukumori, Y., Murata, T., Iwata, S., and Shiro, Y. (2010) Structural Basis of Biological N_2O Generation by Bacterial Nitric Oxide Reductase. *Science (80-.). 330*, 1666–1670.

(50) Moënne-Loccoz, P. (2007) Spectroscopic characterization of heme iron–nitrosyl species and their role in NO reductase mechanisms in diiron proteins. *Nat. Prod. Rep. 24*, 610–620.

(51) Hendriks, J. H. M., Jasaitis, A., Saraste, M., and Verkhovsky, M. I. (2002) Proton and electron pathways in the bacterial nitric oxide reductase. *Biochemistry 41*, 2331–2340.

(52) Blomberg, M. R. A. (2017) Can Reduction of NO to N_2O in Cytochrome *c* Dependent Nitric Oxide Reductase Proceed through a *Trans*-Mechanism? *Biochemistry 56*, 120–131.

(53) Duarte, A. G., Cordas, C. M., Moura, J. J. G., and Moura, I. (2014) Steady-state kinetics with nitric oxide reductase (NOR): new considerations on substrate inhibition profile and catalytic mechanism. *Biochim. Biophys. acta-Bioenergetics 1837*, 375–84.

(54) Cordas, C. M., Duarte, A. G., Moura, J. J. G., and Moura, I. (2013) Electrochemical behaviour of bacterial nitric oxide reductase - Evidence of low redox potential non-heme FeB gives new perspectives on the catalytic mechanism. *Biochim. Biophys. Acta - Bioenerg. 1827*, 233–238.

(55) Speelman, A. L., Zhang, B., Silakov, A., Skodje, K. M., Alp, E. E., Zhao, J., Hu, M. Y., Kim, E., Krebs, C., and Lehnert, N. (2016) Unusual Synthetic Pathway for an {Fe(NO)2}9Dinitrosyl Iron Complex (DNIC) and Insight into DNIC Electronic Structure via Nuclear Resonance Vibrational Spectroscopy. *Inorg. Chem. 55*, 5485–5501.

(56) Girsch, P., and De Vries, S. (1997) Purification and initial kinetic and spectroscopic characterization of NO reductase from *Paracoccus denitrificans*. *Biochim. Biophys. Acta - Bioenerg. 1318*, 202–216.

(57) Moënne-Loccoz, P., and De Vries, S. (1998) Structural characterization of the catalytic high-spin heme b of nitric oxide reductase: A resonance Raman study. *J. Am. Chem. Soc. 120*, 5147–5152.

(58) Kumita, H., Matsuura, K., Hino, T., Takahashi, S., Hori, H., Fukumori, Y., Morishima, I., and Shiro, Y. (2004) NO reduction by nitric-oxide reductase from denitrifying bacterium *Pseudomonas aeruginosa*: Characterization of reaction intermediates that appear in the single turnover cycle. *J. Biol. Chem. 279*, 55247–55254.

(59) Lin, Y., Yeung, N., Gao, Y., Miner, K. D., Tian, S., Robinson, H., and Lu, Y. (2010) Roles of glutamates and metal ions in a rationally designed nitric oxide reductase based on myoglobin. *Proc. Natl. Acad. Sci. U. S. A. 107*, 8581–6.

(60) Chakraborty, S., Reed, J., Sage, J. T., Branagan, N. C., Petrik, I. D., Miner, K. D., Hu, M. Y., Zhao, J., Alp, E. E., and Lu, Y. (2015) Recent Advances in Biosynthetic Modeling of Nitric Oxide Reductases and Insights Gained from Nuclear Resonance Vibrational and Other Spectroscopic Studies. *Inorg. Chem. 54*, 9317–9329.

(61) Matsumura, H., Hayashi, T., Chakraborty, S., Lu, Y., and Moënne-Loccoz, P. (2014) The production of nitrous oxide by the heme/nonheme diiron center of engineered myoglobins (Fe_BMbs) proceeds through a trans -iron-nitrosyl dimer. *J. Am. Chem. Soc. 136*, 2420–2431.

(62) Matsumoto, Y., Tosha, T., Pisliakov, A. V, Hino, T., Sugimoto, H., Nagano, S., Sugita, Y., and Shiro, Y. (2012) Crystal structure of quinol-dependent nitric oxide reductase from *Geobacillus stearothermophilus*. *Nat. Struct. Mol. Biol. 19*, 238–245.

(63) Suharti, Heering, H. A., and de Vries, S. (2004) NO Reductase from *Bacillus azotoformans* Is a Bifunctional Enzyme Accepting Electrons from Menaquinol and a Specific Endogenous Membrane-Bound Cytochrome c_{551} †. *Biochemistry 43*, 13487–13495.

(64) Al-Attar, S., and De Vries, S. (2015) An electrogenic nitric oxide reductase. *FEBS Lett. 589*, 2050–2057.

(65) Park, S., Shimizu, K., Addachi, S., Nakagawa, A., Tanaka, I., Nakahara, K., Shoun, H., Obayashi, E., Nakamura, H., Lizauka, T., and Shiro, Y. (1997) Crystal structure of nitric oxide reductase from denitrifying fungus *Fusarium oxysporum*. *Nature 4*, 827–832.

(66) Lehnert, N., Praneeth, V. K. K., and Paulat, F. (2006) Electronic Structure of Iron(II)-Porphyrin Nitroxyl Complexes: Molecular Mechanism of Fungal Nitric Oxide Reductase (P450nor). *J. Comput. Chem. 27*, 1338–1351.

(67) McQuarters, A. B., Wirgau, N. E., and Lehnert, N. (2014) Model complexes of key intermediates in fungal cytochrome P450 nitric oxide reductase (P450nor). *Curr. Opin. Chem. Biol. 19*, 82–89.

(68) Baillie, T. A. (1981) The Use of Stable Isotopes in Pharmacological Research. *Pharmacol. Rev. 33*, 81–32.

(69) Roeske, C. A., and O'Leary, M. H. (1984) Carbon Isotope Effects on the Enzyme-Catalyzed Carboxylation of Ribulose Bisphosphate. *Biochemistry 23*, 6275–6284.

(70) Huskey, P. W. (1991) Origins and Interpretations of Heavy-Atom Isotope Effects, in *Enzyme Mechanism from Isotope Effects* (Cook, P. F., Ed.), pp 38–70. CRC Press, Inc., Boca Raton.

(71) Lewis, B. E., and Schramm, V. L. (2006) Enzymatic Binding Isotope Effects and the Interaction of Glucose with Hexokinase, in *Isotope Effects in Chemistry and Biology* (Kohen, A., and Limbach, H.-H., Eds.), pp 1020–1050. CRC Press, Inc., New York.

(72) Westheimer, F. H. (1961) The magnitude of the primary kinetic isotope effect for compounds of hydrogen and deuterium. *Chem. Rev. 61*, 265–273.

(73) Forster, P., V. Ramaswamy, P. Artaxo, T. Berntsen, R. Betts, D.W. Fahey, J. Haywood, J. Lean, D.C. Lowe, G. Myhre, J. Nganga, R. P., and G. Raga, M. S. and R. V. D. (2007) Changes in Atmospheric Constituents and in Radiative Forcing, in *Climate Change 2007: The Physical Science Basis. Contribution of Working Group I to the Fourth Assessment Report of the Intergovernmental Panel on Climate Change* (Solomon, S., D. Qin, M. Manning, Z. Chen, M. Marquis, K.B. Averyt, M. T. and H. L. M., Ed.), pp 131–217. Cambridge University Press, New York.

(74) Crow, A., Matsuda, Y., Arata, H., and Oubrie, A. (2016) Structure of the Membrane-intrinsic Nitric Oxide Reductase from *Roseobacter denitrificans*. *Biochemistry 55*, 3198–3203.

(75) Shiro, Y., Sugimoto, H., Tosha, T., Nagano, S., and Hino, T. (2012) Structural basis for nitrous oxide generation by bacterial nitric oxide reductases. *Source Philos. Trans. Biol. Sci. 367*, 1195–1203.

(76) Schneider, J. L. (2011) How Kinetic Isotope Effects Can Be Used to Understand Enzymatic Transition States. *Einstein J. Biol. Med. 27*, 18–19.

(77) Flock, U., Watmough, N. J., and Ädelroth, P. (2005) Electron/proton coupling in bacterial nitric oxide reductase during reduction of oxygen. *Biochemistry 44*, 10711–10719.

(78) Toyoda, S., and Yoshida, N. (1999) Determination of nitrogen isotopomers of nitrous oxide on a modified isotope ratio mass spectrometer. *Anal. Chem. 71*, 4711–4718.

(79) Yu, C., and Yao, W. (2017) Robust linear regression: A review and comparison. *Commun. Stat. - Simul. Comput. 46*, 6261–6282.

(80) O'Leary, M. H. (1989) Multiple isotope effects on enzyme-catalyzed reactions. *Annu. Rev. Biochem. 58*, 377–401.

(81) Singh, P., Islam, Z., and Kohen, A. (2016) Examinations of the Chemical Step in Enzyme Catalysis. *Methods Enzymol.* 1st ed. Elsevier Inc.

(82) Toyoda, S., Yoshida, N., and Koba, K. (2017) Isotopocule Analysis of Biologically Produced Nitrous Oxide in Various Environments. *Mass Spectrom. Rev. 36*, 135–160.

(83) Kool, D. M., Wrange, N., Oenema, O., Dolfing, J., and Van Groenigen, J. W. (2007) Oxygen exchange between (de)nitrification intermediates and H_2O and its implications for source determination of NO_3^- and N_2O: a reviw. *Rapid Commun. Mass Spectrom. 21*, 3569–3578.

(84) Averill, B. A. (1996) Dissimilatory nitrite and nitric oxide reductases. *Chem. Rev. 96*, 2951–2964.

(85) Rex, D., Clough, T. J., Richards, K. G., de Klein, C., Morales, S. E., Samad, M. S., Grant, J., and Lanigan, G. J. (2018) Fungal and bacterial contributions to codenitrification emissions of N_2O and N_2 following urea deposition to soil. *Nutr. Cycl. Agroecosystems 110*, 135–149.

(86) Yamazaki, T., Hozuki, T., Arai, K., Toyoda, S., Koba, K., Fujiwara, T., and Yoshida, N. (2014) Isotopomeric characterization of nitrous oxide produced by reaction of enzymes extracted from nitrifying and denitrifying bacteria. *Biogeosciences 11*, 2679–2689.

(87) Blomberg, L. M., Blomberg, M. R. A., and Siegbahn, P. E. M. (2006) Reduction of nitric oxide in bacterial nitric oxide reductase-a theoretical model study. *Biochim. Biophys. Acta - Bioenerg. 1757*, 240–252.

(88) Hendriks, J. H. M., Jasaitis, A., Saraste, M., and Verkhovsky, M. I. (2002) Proton and electron pathways in the bacterial nitric oxide reductase. *Biochemistry 41*, 2331–2340.

(89) Yeung, N., Lin, Y. W., Gao, Y., Zhao, X., Russell, B., Lei, L., Miner, K. D., Robinson, H., and Lu, Y. (2009) Rational design of a structural and functional nitric oxide reductase. *Nature 462*, 1079–1081.

(90) Cleland, W. W. (2005) The use of isotope effects to determine enzyme mechanisms. *Arch. Biochem. Biophys. 433*, 2–12.

(91) Berto, T. C., Hoffman, M. B., Murata, Y., Landenberger, K. B., Alp, E. E., Zhao, J., and Lehnert, N. (2011) Structural and electronic characterization of non-heme Fe(II)-nitrosyls as biomimetic models of the Fe_B center of bacterial nitric oxide reductase. *J. Am. Chem. Soc. 133*, 16714–16717.

(92) Tsubaki, M., and Yu, N. T. (1982) Resonance Raman Investigation of Nitric Oxide Bonding in Nitrosylhemoglobin A and -myoglobin: Detection of Bound N-O Stretching and Fe-NO Stretching Vibrations from the Hexacoordinated NO-Heme Complex. *Biochemistry 21*, 1140–1144.

(93) Burton, G. W., Sims, L. B., Wilson, J. C., and Fry, A. (1977) Calculation of Carbon-14, Chlorine-37, and Deuterium Kinetic Isotope Effects in the Solvolysis of tert-Butyl Chloride. *J. Am. Chem. Soc. 99*, 3371–3379.

(94) Williams, R. C., and Taylor, J. W. (1974) Chlorine kinetic isotope effect models. II. Vibrational analysis and KIE [kinetic isotope effects] calculations of tert-butyl chloride transition state models. *J. Am. Chem. Soc. 96*, 3721–3727.

(95) Davidson, E. A., and Kanter, D. (2014) Inventories and scenarios of nitrous oxide emissions. *Environ. Res. Lett. 9*, 1–12.

(96) Matsumura, H., Chakraborty, S., Reed, J., Lu, Y., and Moënne-Loccoz, P. (2016) Effect of Outer-Sphere Side Chain Substitutions on the Fate of the trans Iron-Nitrosyl Dimer in Heme/Nonheme Engineered Myoglobins (Fe_BMbs): Insights into the Mechanism of Denitrifying NO Reductases. *Biochemistry 55*, 2091–2099.

(97) Chakraborty, S., and Reed, J. (2014) Spectroscopic and Computational Study of a Non-heme Iron- Nitrosyl Center in a Biosynthetic Model of Nitric Oxide Reductases in Myoglobin Containing Zn-protoporphyrin IX: Support for the *Trans* Mechanism of NO Reduction Saumen. *Angew Chem Int Ed Engl 53*, 2417–2421.

(98) Hogg, N., and Kalyanaraman, B. (1998) The Use of NO Gas in Biological Systems, in *Nitric Oxide Protocols* (Walker, J. M., and Titheradge, M. A., Eds.), pp 231–236. Humana Press Inc., Totowa, New Jersey.

(99) Fox, J. B. J., and Ackerman, S. A. (1968) Formation of Nitric Oxide Myoglobin : *J. Food Sci. 33*, 364–370.